Lithosphere

Research Article

Evolution of Subduction Dynamics beneath West Avalonia in Middle to Late Ordovician Times

Pierre Jutras ⓘ,[1] **J. Brendan Murphy,**[2] **Dennis Quick,**[1] **and Jaroslav Dostal**[1]

[1]*Department of Geology, Saint Mary's University, Halifax, NS, Canada B3H 3C3*
[2]*Department of Earth Sciences, St. Francis Xavier University, P.O. Box 5000, Antigonish, NS, Canada B2G 2W5*

Correspondence should be addressed to Pierre Jutras; pierre.jutras@smu.ca

Middle to Upper Ordovician volcanic rocks in the Arisaig area of Nova Scotia, Canada, constitute the only known record of volcanism in West Avalonia during that interval. Hence, they have been extensively studied to test paleocontinental reconstructions that consistently show Avalonia as a drifting microcontinent during that period. Identification of volcanic rocks with an intermediate composition (the new Seaspray Cove Formation) between upper Darriwilian bimodal volcanic rocks of the Dunn Point Formation and Sandbian felsic pyroclastic rocks of the McGillivray Brook Formation has led to a reevaluation of magmatic relationships in the Ordovician volcanic suite at Arisaig. Although part of the same volcanic construction, the three formations are separated by significant time-gaps and are shown to belong to three distinct magmatic subsystems. The tectonostratigraphic context and trace element contents of the Dunn Point Formation basalts suggest that they were produced by the high-degree partial melting of an E-MORB type source in a back-arc extensional setting, whereas trace element contents in intermediate rocks of the Seaspray Cove Formation suggest that they were produced by the low-degree partial melting of a subduction-enriched source in an arc setting. The two formations are separated by a long interval of volcanic quiescence and deep weathering, during which time the back-arc region evolved from extension to shortening and was eventually onlapped by arc volcanic rocks. Based on limited field constraints, paleomagnetic and paleontological data, this progradation of arc onto back-arc volcanic rocks occurred from the north, where an increasingly young Iapetan oceanic plate was being subducted at an increasingly shallow angle. Partial subduction of the Iapetan oceanic ridge is thought to have subsequently generated slab window magmatism, thus marking the last pulse of subduction-related volcanism in both East and West Avalonia.

1. Introduction

Paleozoic continental and plate reconstructions indicate that the composite microcontinent of Avalonia rifted away from Gondwana in the Early Ordovician, opening the Rheic Ocean, and drifted northward towards Laurentia during the rest of the Ordovician, gradually closing the Iapetus Ocean [1–7]. As such, its evolution constrains events leading to the amalgamation of Pangea (e.g., [8]). The area of Arisaig, Nova Scotia, Canada (Figure 1), includes the only known succession of Middle to Upper Ordovician volcanic rocks in West Avalonia (i.e., the North American portion of Avalo-

nia) and has been extensively studied to shed light on the tectonic and paleogeographic history of the terrane during this pivotal time interval (e.g., [9–15]). Until recently, only mafic and felsic volcanic rocks were known from that locality and were interpreted as the bimodal products of back-arc extension [13–15]. This paper describes the Seaspray Cove Formation, a newly identified >35 m thick succession of volcanic rocks with an intermediate chemical composition within the Ordovician succession at Arisaig, and discusses the implications of its geochemistry. Based on comparisons with bounding volcanic units of the Middle Ordovician Dunn Point Formation and Upper Ordovician McGillivray Brook
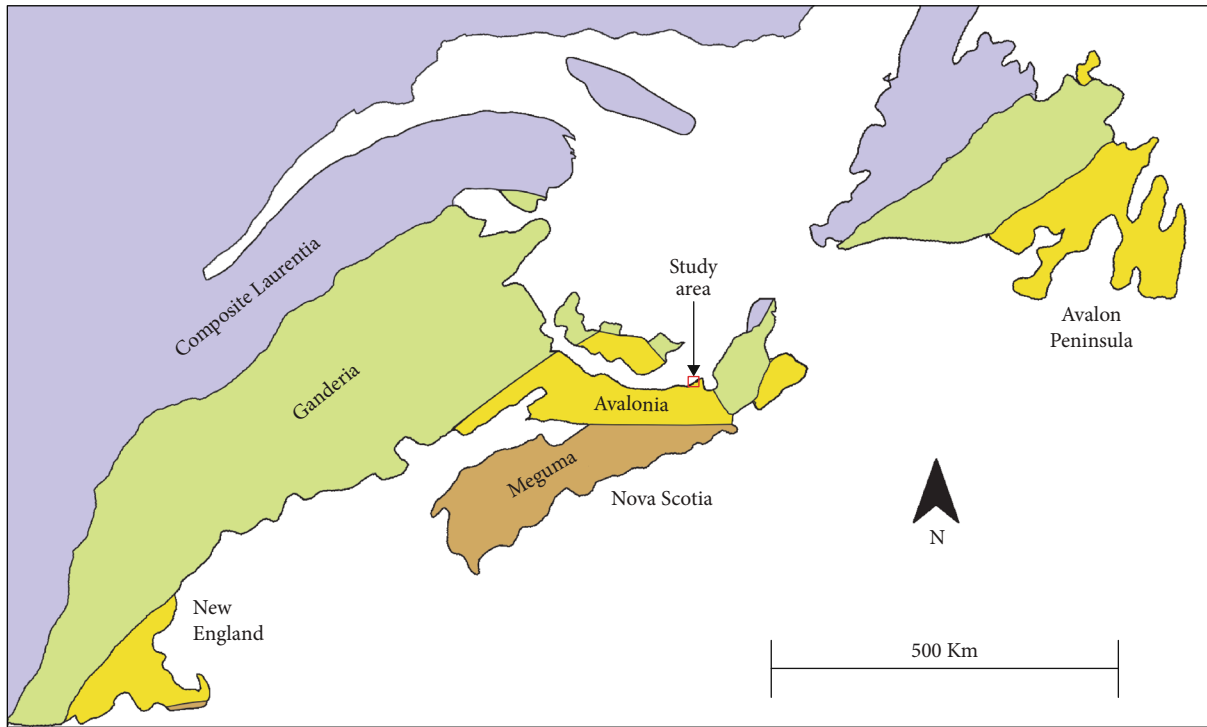
(a)
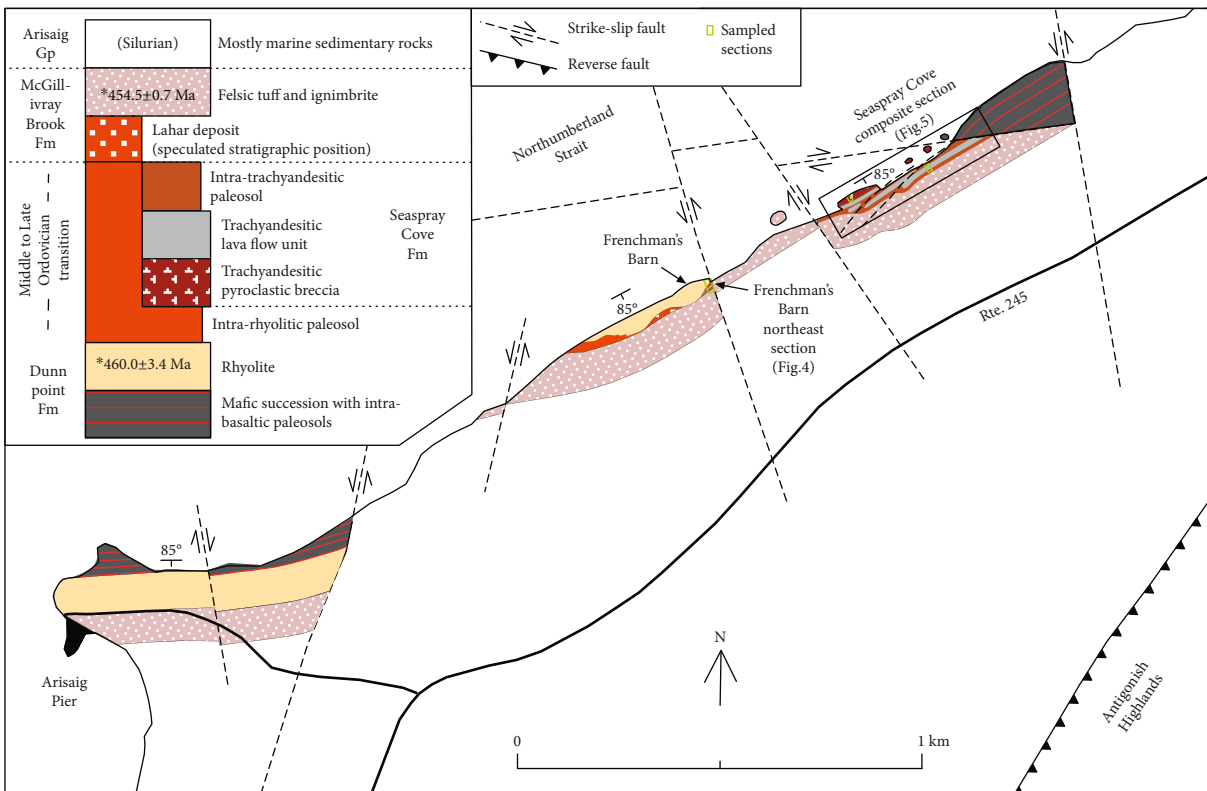
(b)

Figure 1: (a) Map of northeastern North America showing the major lithotectonic units of the Appalachian-Caledonian orogenic belt (modified after [23, 68]), as well as the location of the study area within Avalonia. (b) Generalized geology of the study area with localities of the sampled sections (green rectangles).

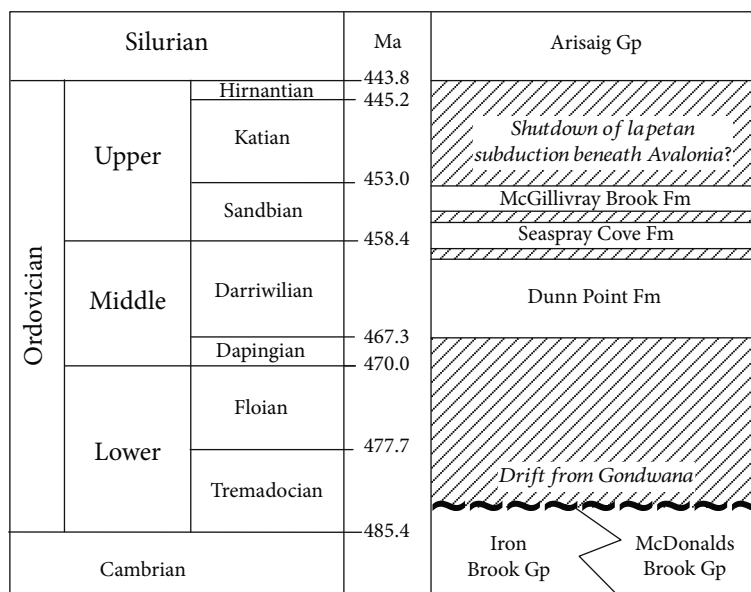| Silurian			Ma	Arisaig Gp

FIGURE 2: Lower to middle Paleozoic stratigraphy of the Arisaig area in northern Nova Scotia (time scale after [69]) based on Hamilton and Murphy [9], Murphy et al. [14, 16], and this study.

Formation, as well as on parallels with coeval units of correlative terranes in the British Isles, this paper proposes an integrated geodynamic model for the evolution of Middle to Late Ordovician subduction-related volcanism in West Avalonia.

2. Geological Setting

Basement rock exposures near the study area are characterized by Neoproterozoic arc-related volcanic and sedimentary rocks (Georgeville Group) truncated by Ediacaran plutonic rocks [15, 16], which are unconformably overlain by a Cambrian to Lower Ordovician succession of sedimentary rocks that contain fauna diagnostic of Avalonia (e.g., [17, 18]). Following an Early Ordovician episode of compressive deformation [11, 16] and subsequent rifting from Gondwana [3], Middle to Upper Ordovician volcanic rocks of the Dunn Point and McGillivray Brook Formations [19, 20] were emplaced on the drifting microcontinent of Avalonia [6, 14] (Figure 2). Based on U-Pb isotopes from primary zircons, Hamilton and Murphy [9] obtained a 460.0 ± 3.4 Ma age (upper Darriwilian/Llanvirnian) for rhyolite of the Dunn Point Formation, and Murphy et al. [14] subsequently dated the top ignimbrite of the overlying McGillivray Brook Formation at 454.5 ± 0.7 Ma (Sandbian/Caradoc) with the same method, providing an upper limit to the age of the volcanic succession at Arisaig (Figure 2). The newly identified Seaspray Cove Formation is undated, but stratigraphically positioned between these two units, and therefore constrained between ~460 and ~454.5 Ma (Figure 2).

Paleomagnetic data [10] adapted to subsequent geochronological data place the volcanic rocks of Arisaig at a paleolatitude of $41° \pm 5°$ south at ~460 Ma [9]. Paleogeographic reconstructions for that time interval show the Avalonian and Ganderian microcontinents drifting northward on the same microplate, possibly separated by a narrow seaway, with the Rheic Ocean separating them from Gondwana to the south, and the Iapetus Ocean separating them from Laurentia to the north [1, 6, 8]. This drift is consistent with the paleolatitude of $32° \pm 8°$ south determined by Hodych and Buchan [21] for West Avalonia at ~440 Ma (Early Silurian) based on paleomagnetic data from the Cape St. Mary's sills (U-Pb baddeleyite age of $441 + 2$ Ma; [22]) on the Avalon Peninsula of Newfoundland (Figure 1(a)). Based on the Ordovician geology of Avalonian and Ganderian sequences in Ireland, Great Britain and eastern North America, this northward migration was accommodated by subduction of the Iapetan oceanic lithosphere to the north beneath Laurentia, and to the south beneath Avalonia and Ganderia ([5, 7]; van Staal et al. 1998, [8, 15, 23]).

3. Previous Work on the Ordovician Volcanic Successions at Arisaig

Between the localities of Arisaig Pier and Frenchman's Barn (a monadnock of resistant rhyolite that is reinforced by quartz veinlets; Figure 1(b)), the Seaspray Cove Formation is absent, and the Dunn Point Formation is directly overlain by the McGillivray Brook Formation (Figure 3).

3.1. The Dunn Point Formation and Intrusive Equivalents. The Dunn Point Formation is a succession of mafic flows separated by weathering profiles and topped by a thick rhyolite flow, which also hosts a thick paleosol [19, 24–26] (Figures 1(b)–1(c) and 3). Keppie et al. [20] attributed the Dunn Point Formation basalts to a within-plate, continental rifting event, but based on inferences made with the Ordovician geology of East Avalonia, Murphy et al. [13, 14] more specifically associated the volcanism to ensialic back-arc spreading analogous to the Lau-Havre-Taupo system of
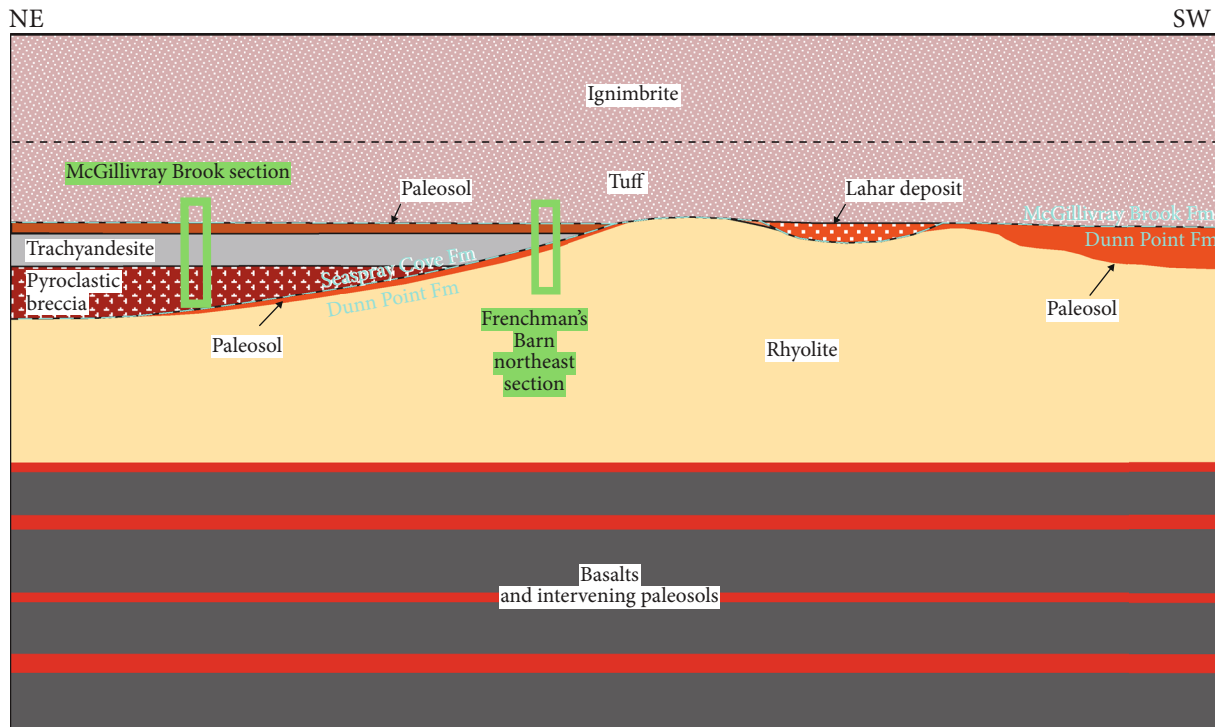
FIGURE 3: Schematic cross-section of the Ordovician succession at Arisaig prior to its subsequent faulting (not to scale). The contact relationships are based on available exposures in the extended study area of Jutras et al. [26]. Legend in Figure 1.

New Zealand, with mafic magmatism resulting from decompression melting of the underlying mantle.

The ~70 m thick overlying flow-banded rhyolite has a composition analogous to A-type, within-plate granites and is interpreted as a product of crustal anatexis generated by heat derived from the associated mafic melt [14]. Based on Sm–Nd isotopic data, these felsic rocks were sourced from Avalonian lower crust [15].

Bimodal plutons with correlative geochemical signatures are found in the Antigonish Highlands (Figure 1(b)), less than 50 km south of the Dunn Point Formation exposures [27]. This plutonic suite records a longer history of within-plate bimodal magmatism dating back to the Early Ordovician rifting of Avalonia from Gondwana. Based on Sm–Nd isotopic data, the intrusive felsic rocks were also sourced from Avalonian lower crust [15].

As noted earlier, the upper part of the Dunn Point Formation rhyolite is extensively weathered [26]. Exposed sections of this intra-rhyolitic paleosol are up to 8.5 m thick, but based on strain calculations (*sensu* [28]), this probably represents ~30% of its original thickness prior to burial compaction [24]. This thick paleosol is the record of a long period of magmatic inactivity that followed the massive eruption of rhyolite.

3.2. The McGillivray Brook Formation. Disconformably overlying the Dunn Point Formation to the southwest of Frenchman's Barn (Figure 1(b)), the McGillivray Brook Formation is mainly characterized by pyroclastic and volcaniclastic deposits. Its base shows discontinuous lenses of lahar deposits, which locally truncate the thick paleosol that tops the Dunn Point Formation rhyolite (Figures 1(b) and 3). These basal lenses of lahar deposits, as well as the knobs of weathered rhyolite that laterally separate them, are directly overlain by a succession of felsic lapilli tuff that transitions upward into felsic ignimbrite with an A-type composition [14, 19]. Based on Sm–Nd isotopic data, this felsic pyroclastic succession was sourced from Avalonian lower crust, but from presumably drier melting and at much higher temperature (1050°C) than the Dunn Point Formation rhyolite (860 to 875°C) according to zircon saturation thermometry estimates [15]. As zircon dissolves between 750 and 850°C under pressures typical of the lower crust [29], the high temperature estimates for crustal melting may also explain its much higher content in high-field-strength elements compared to rhyolites of the Dunn Point Formation.

4. The New Seaspray Cove Formation

An incomplete succession of intermediate pyroclastic breccia and lava flow units (classified below as trachyandesitic) pinches in-between the localities of Frenchman's Barn and Seaspray Cove (informal toponym; Figure 1(b)), disconformably above the Dunn Point Formation, and conformably below the McGillivray Brook Formation (Figure 3). Because these lithologies are not included in the definition of the Dunn Point and McGillivray Brook Formations, they are herein formalized as the new Seaspray Cove Formation. The type-area is on the Northumberland Straight shoreline,
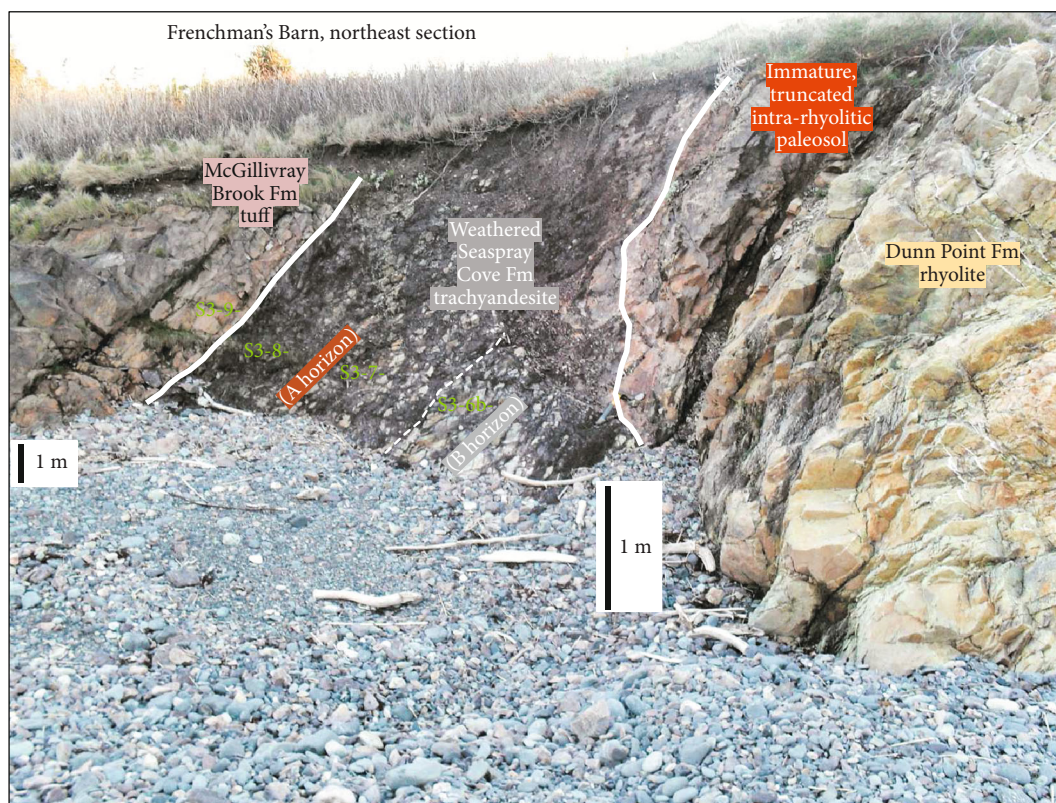
FIGURE 4: Weathered and sheared trachyandesite of the Seaspray Cove Formation truncating weathered rhyolite of the Dunn Point Formation, and conformably overlain by tuff of the McGillivray Brook Formation at the Frenchman's Barn northeast section (locality shown in Figure 1). View towards the southwest. Sample localities are indicated. Modified from Jutras et al. [26].

to the southwest of Seaspray Lane in the municipality of Arisaig (Figure 1(b)).

On the northeast flank of Frenchman's Barn (Figure 1(b)), the pyroclastic breccia is absent, and an up to ~4.5 m thick weathered lava flow unit of the Seaspray Cove Formation disconformably truncates the weathered rhyolite and is conformably overlain by the lowermost tuff of the McGillivray Brook Formation (Figures 3 and 4). Based on evidence of mixing between weathered rhyolite and trachyandesitic material at the base of the massive, intermediate flow [26], the latter partly bulldozed and incorporated weathered rhyolitic material during emplacement. According to these authors, the truncated rhyolite paleosol at this locality is considerably less well-developed than the southwest of Frenchman's Barn, where that paleosol is directly overlain by tuff of the McGillivray Brook Formation, with no intervening intermediate rocks of the Seaspray Cove Formation (Figure 3).

To the northeast, along Seaspray Cove (Figure 1(b)), the trachyandesite lava flow unit is at least 15 m thick (weathering and shearing in its upper part altered its original thickness) and is poorly weathered in its basal ~11.5 m, but thoroughly weathered above that level. Postemplacement thrust faulting was concentrated in this weak upper interval of deeply weathered material, which resulted in local duplications of the more competent lower interval (Figure 5). At the Seaspray Cove locality, the trachyandesitic lava flow unit lies concordantly above dark red pyroclastic breccia of the same formation, and concordantly below the McGillivray Brook Formation felsic tuff and ignimbrite (Figures 3 and 5). The base of the breccia is not exposed, but it is at least 20 m thick based on available exposure. The thickness and nature of strata that separate this incompletely exposed succession from the underlying Dunn Point Formation are unknown, but as it pinches-out at a short distance to the southwest, it is inferred that the breccia directly overlies the weathered rhyolite (Figure 3).

The newly identified trachyandesitic flow unit was mistakenly assigned by previous authors (e.g., [13, 14, 19]) to the basaltic succession of the underlying Dunn Point Formation, which is in fault contact with it at the Seaspray Cove locality (Figure 5). Both units look similar in outcrop, although the Dunn Point Formation basalts are darker. Based on field observations, the pyroclastic breccia that underlies the trachyandesite was previously confused for a lahar deposit [13, 19, 26]. However, this unit is considerably darker, denser, less matrix-rich, and much richer in mobile elements than lahar deposits that truncate the intrarhyolitic paleosol in other areas.

5. Analytical Methods

Two samples were obtained from pyroclastic breccia of the Seaspray Cove Formation, and 10 samples were retrieved
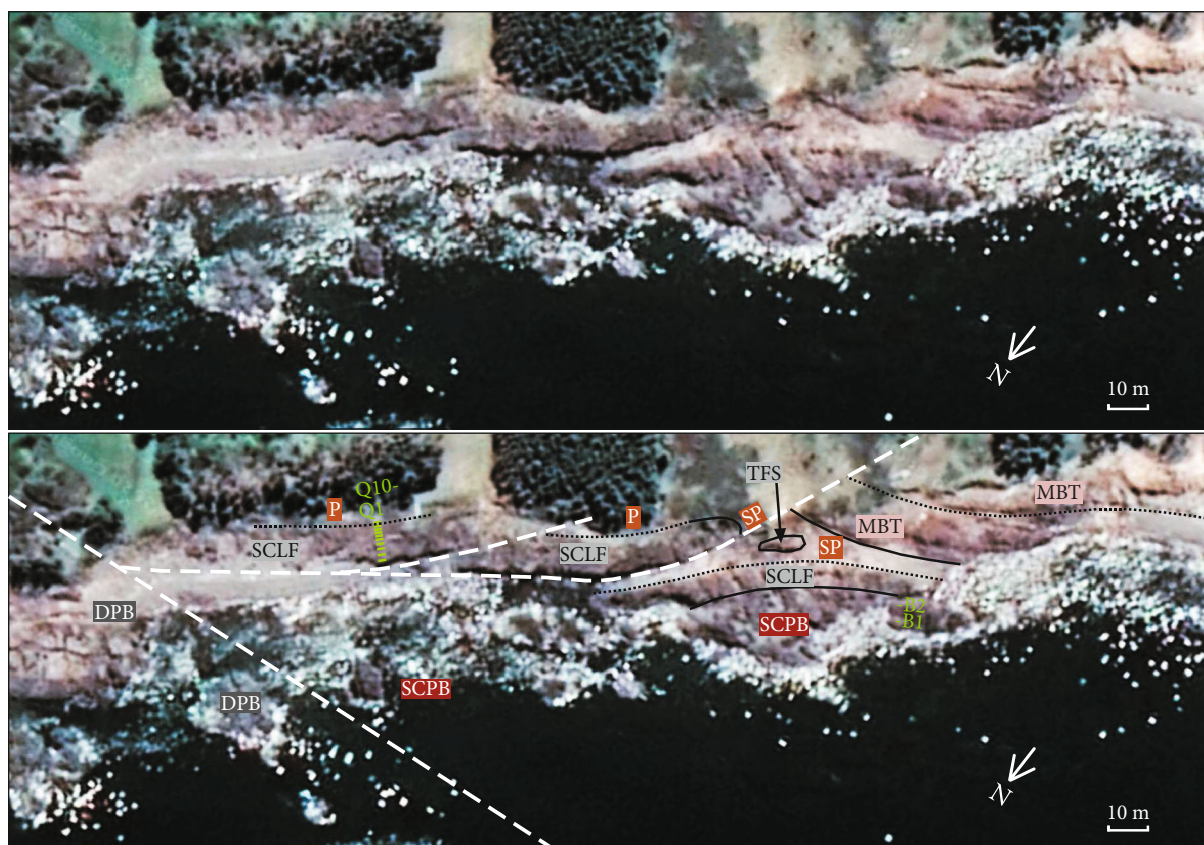
FIGURE 5: Field relationships between pyroclastic breccia and lava flow units of the Seaspray Cove Formation and tuff of the McGillivray Brook Formation at the Seaspray Cove locality (shown in Figure 1). Postdeposition faulting concentrated in the weak, weathered upper part of the trachyandesitic lava flow unit, which resulted in local duplications of its more competent base. Sample localities are indicated. DPB: Dunn Point Formation basalt; SCPB: Seaspray Cove Formation pyroclastic breccia; SCLF: Seaspray Cove Formation trachyandesitic lava flow unit; P: paleosol; SP: sheared paleosol and fault breccia; TFS: trachyandesite fault slab; MBT: McGillivray Formation tuff; MBI: McGillivray Formation ignimbrite. The satellite image is from Google Maps.

from the overlying lava flow unit at irregular intervals at Seaspray Cove (B1-2 and Q1-10 on Figure 5). Sampling was performed at shorter intervals in the upper part of the profile in order to precisely determine the downward extent of subsurface Ordovician weathering and to assess element mobility during weathering. Three additional samples were obtained at regular intervals from the ~4.5 m thick trachyandesite at the Frenchman's Barn northeast section, two of which were included in Jutras et al. [26]. Thin-sections were made for all samples, and part of each was powdered for mineralogical and geochemical analyses. Results of X-ray diffraction (XRD) analyses are shown in Table 1; X-ray fluorescence (XRF) data for major and selected trace elements are shown in Table 2; and inductively coupled plasma mass spectrometry (ICP-MS) data for a broader list of trace elements are shown in Table 3. Tables 1–3 also include data from Keppie et al. [12], Murphy et al. [14], and Jutras et al. [25, 26] on the least altered and least contaminated samples (based on high Na_2O and low LOI contents) of basalts and rhyolite of the Dunn Point Formation, as well as from lahar, tuff and ignimbrite deposits of the McGillivray Brook Formation.

All lava flow unit samples of the Seaspray Cove type-section, except the thoroughly weathered Q10 (plagioclase contents fully altered to secondary minerals; Table 1), were analyzed for their total carbon, chlorine and fluorine contents, as determined by combustion analysis, instrumental neutron activation analysis (INAA) and fusion/ion-selective electrode (Fus-ISE), respectively, (Table 4). Furthermore, element mapping by X-ray fluorescence was performed on sample B2 of the pyroclastic breccia with a Bruker M4 Tornado micro-XRF housed at the University of New Brunswick in Fredericton, Canada (Figure 6). Twenty points from a non-oxidized portion of the matrix were analyzed for major element contents with an electron microprobe (Data Repository File #1), and for trace element contents with a laser ablation inductively coupled plasma mass spectrometer (LA-ICP-MS) (Data Repository File #2), also housed at the University of New Brunswick.

6. Petrology of the Trachyandesitic Lava Flow Unit

6.1. Petrography. In its basal ~8 m at Seaspray Cove (samples Q1-4), the newly identified intermediate lava flow unit is

TABLE 1: Mineralogy of pyroclastic breccia and trachyandesite of the Seaspray Cove Formation and lahar of the McGillivray Brook Formation.

Lithology	Sample	Distance From base:	Albite Vol.%	Orthoclase Vol.%	Quartz Vol.%	Clinochlore Vol.%	Muscovite Vol.%	Pyrophyllite Vol.%	Calcite Vol.%	Dolomite Vol.%	Siderite Vol.%	Ankerite Vol.%	Hematite Vol.%	Amorphous Vol.%
Frenchman's Barn northeast section:														
SC tra. A hor.	S3-8	3.5 m		9	32		28	3					28	
SC tra. A hor.	S3-7	2.5 m		6	45		26	2					21	
SC tra. B hor.	S3-6b	1.5 m	5	1	71	4	18						1	
Seaspray Cove composite section:														
SC tra. B hor.	Q10	11.75 m		3	76	5	9						6	
SC tra. C hor.	Q9	11.5 m	42	6	32	7	8		2				3	
SC tra. C hor.	Q8	11.25 m	34	4	28	8	16						8	
SC tra. C hor.	Q7	11 m	42	4	24	9	4		7	2	1	1	7	
SC tra. C hor.	Q6	10 m	19	3	60	10	4		1	1		1	1	
SC tra. C hor.	Q5	9 m	28	8	44	9	4		4			1	2	
SC tra. R hor.	Q4	7 m	38	7	31	14	4		4			1	1	
SC tra. R hor.	Q3	5 m	36	7	35	14	2		4			2	1	
SC tra. R hor.	Q2	3 m	38	7	31	15	2		6				1	
SC tra.	Q1	0.5 m	45	6	24	17	1		5	1	1		1	
		from top:												
SC pyr-br.	B2	7 m	14	1	67	4	5						7	3
SC pyr-br.	B1	15 m	8	1	70	3	6						8	4
McG lahar	BRL		2		35		54						9	

Note: determined by X-ray diffraction performed at the Département des Science de la Terre et de l'Atmospshère de l'Université du Québec à Montréal, Canada, using a Siemens D5000 diffractometer. Samples S3-7 and S3-8 are from the Frenchman's Barn northeast section Jutras et al. [26]. McG: McGillivray Brook Formation; SC; Seaspray Cove Formation; tra.: trachyandesite; pyr-br.: pyroclastic breccia; hor.: horizon.

TABLE 2: Whole-rock major element and Zr, Y, and Nb contents in the various lithologies of the Dunn Point, Seaspray Cove, and McGillivray Brook Formations.

Lithology	Sample	Interval	SiO$_2$ (Wt.%)	TiO$_2$ (Wt.%)	Al$_2$O$_3$ (Wt.%)	Fe$_2$O$_3$ (Wt.%)	MnO (Wt.%)	MgO (Wt.%)	CaO (Wt.%)	Na$_2$O (Wt.%)	K$_2$O (Wt.%)	P$_2$O$_5$ (Wt.%)	LOI (Wt.%)	Total (Wt.%)	Nb (ppm)	Y (ppm)	Zr (ppm)
Seaspray Cove composite section: [This study]		Dist. from base															
(SC tra. B hor.)	Q10	11.75 m	65.6	1.9	13.1	11.2	0.1	0.7	0.4	0.1	3.9	0.3	2.9	100.2	51	65	462
(SC tra. C hor.)	Q9	11.5 m	63.2	2.1	14.9	6.8	0.3	0.8	2.3	3.5	2.3	0.9	2.8	99.9	56	59	525
(SC tra. C hor.)	Q8	11.25 m	47.1	2.8	20.1	15.6	0.2	0.8	1.8	2.3	5.0	1.2	3.4	100.3	73	103	682
(SC tra. C hor.)	Q7	11 m	50.2	1.9	15.7	13.5	0.3	0.8	5.1	3.9	2.4	0.9	5.4	100.1	52	81	490
(SC tra. C hor.)	Q6	10 m	63.0	1.9	13.4	10.0	0.3	1.3	2.0	1.3	2.4	0.8	3.6	100.0	50	58	479
(SC tra. C hor.)	Q5	9 m	61.3	1.9	13.8	9.1	0.2	0.7	3.3	2.6	2.4	0.8	3.7	99.9	51	58	494
(SC tra. R hor.)	Q4	7 m	54.3	2.1	14.6	10.0	0.3	1.2	6.0	3.4	1.7	0.9	5.7	100.1	55	64	530
(SC tra. R hor.)	Q3	5 m	55.6	2.0	14.6	9.4	0.3	1.4	4.9	4.2	1.2	0.9	4.9	99.3	54	65	526
(SC tra. R hor.)	Q2	3 m	53.2	2.0	14.5	10.4	0.3	1.7	5.5	3.8	1.1	0.8	5.7	99.0	55	60	544
(SC tra.)	Q1	0.5 m	53.3	2.1	15.3	11.9	0.5	1.7	4.2	4.3	0.4	0.9	4.7	99.2	61	66	565
		Dist. from top:															
SC pyr-br.	B2	7 m	69.3	0.5	12.2	8.0	0.2	0.8	1.5	2.1	2.6	0.1	2.9	100.0	36	49	398
SC pyr-br.	B1	15 m	66.5	0.8	13.4	8.7	0.1	0.8	1.6	2.0	2.9	0.2	3.5	100.4	69	81	738
Frenchman's Barn northeast section:																	
Juttras et al. [26]		Dist. from base															
McG tuff	S3-9	0.25 m	76.5	0.3	12.8	2.8	0.0	0.3	0.0	0.1	4.1	0.1	2.9	99.9	106	241	1971
Juttras et al. [26]		Dist. from top															
McG tra. A hor.	S3-8	1 m	42.5	3.0	22.1	17.4	0.0	0.4	1.2	0.2	7.2	0.9	5.3	100.1	88	135	889
McG tra. A hor.	S3-7	2 m	46.1	2.9	21.3	14.6	0.0	0.4	1.3	0.1	7.0	1.0	5.5	100.4	74	112	823
McG tra. B hor.	S3-6b	3 m	66.36	2.067	15.43	5.84	0.049	0.35	1.25	0.43	5.18	0.92	2.54	100.4	55.7	81.9	520
Dunn Pt rhyolite	S3-1	6 m	81.15	0.148	10.64	0.3	0.004	0.06	0.06	3.72	3.1	0.03	0.61	99.92	42.9	87.3	357
Frenchman's Barn southwest section:																	
Murphy et al. [14]																	
McG ignimbrite	BL08-2		75.4	0.2	12.0	3.3	0.0	0.2	0.1	1.8	6.5	0.0	0.5	100.0	176	198	1914
McG ignimbrite	BL08-3		76.5	0.2	11.4	3.4	0.0	0.1	0.1	2.2	5.8	0.0	0.3	100.0	138	154	1492
McG ignimbrite	BL08-4		76.8	0.2	11.7	2.2	0.0	0.1	0.1	2.0	6.5	0.0	0.4	99.9	126	158	1629
McG ignimbrite	BL08-5		76.9	0.2	11.7	2.7	0.0	0.2	0.1	2.0	5.5	0.0	0.7	100.0	126	156	1548
Juttras et al. [26]																	
McG tuff	S1-20		65.5	0.7	16.6	7.1	0.0	0.3	0.1	0.1	5.2	0.1	3.8	99.5	189	269	2264
McG tuff	S1-19		57.1	0.8	22.5	4.9	0.0	0.4	0.1	0.1	6.5	0.1	6.9	99.4	283	329	3221
McG. lahar	BRL		51.6	0.4	29.4	6.2	0.0	0.1	0.0	0.2	7.4	0.0	4.5	99.8	121	54	1098
Dunn Pt rhyolite	S1-1		73.7	0.2	15.3	1.0	0.0	0.1	0.1	5.6	2.9	0.0	1.1	100.0	60	72	495
Arisaig Pier to Frenchman's Barn:																	

TABLE 2: Continued.

Lithology	Sample	Interval	SiO$_2$ (Wt.%)	TiO$_2$ (Wt.%)	Al$_2$O$_3$ (Wt.%)	Fe$_2$O$_3$ (Wt.%)	MnO (Wt.%)	MgO (Wt.%)	CaO (Wt.%)	Na$_2$O (Wt.%)	K$_2$O (Wt.%)	P$_2$O$_5$ (Wt.%)	LOI (Wt.%)	Total (Wt.%)	Nb (ppm)	Y (ppm)	Zr (ppm)
Murphy [14]																	
Dunn Pt rhyolite	DPF-02		73.1	0.3	14.6	2.4	0.0	0.1	0.1	4.4	5.6	0.0	0.3	101.0	63	58	488
Dunn Pt rhyolite	DPF-04		72.4	0.3	14.2	3.2	0.0	0.1	0.1	4.5	5.1	0.0	0.6	100.5	65	63	505
Dunn Pt rhyolite	DPF-05		74.1	0.3	14.1	2.8	0.0	0.1	0.1	4.4	5.1	0.0	0.5	101.5	65	105	487
Dunn Pt rhyolite	DPF-06		76.0	0.2	13.5	2.0	0.0	0.1	0.1	4.2	5.0	0.0	0.5	101.7	61	57	469
Jutras et al. [25]																	
Dunn Pt basalt	A5a		47.2	2.7	16.4	15.8	0.2	4.4	3.3	4.8	0.7	0.5	4.4	100.5	16	23	152
Dunn Pt basalt	A4a		44.8	2.4	16.6	14.3	0.4	5.9	7.2	3.9	0.7	0.4	4.0	100.7	13	21	131
Dunn Pt basalt	A3a		48.5	2.6	15.9	13.2	0.4	6.3	2.6	4.9	0.4	0.4	5.8	100.8	15	25	141
Dunn Pt basalt	A2a		47.8	2.1	17.4	12.7	0.4	7.1	1.0	5.6	0.3	0.3	5.3	99.9	17	26	158
Dunn Pt basalt	DB2a		48.7	2.5	16.5	13.0	0.2	6.7	3.2	3.9	0.4	0.4	4.6	100.1	18	34	174
Dunn Pt basalt	DB1a		48.9	2.5	15.6	15.2	0.2	6.5	2.6	3.4	0.1	0.4	5.4	100.6	18	28	164
Dunn Pt basalt	M2a		43.3	2.8	18.1	16.4	0.2	7.1	2.0	4.5	0.4	0.5	5.6	100.8	20	34	194
Dunn Pt basalt	M1a		46.6	2.3	14.6	15.9	0.3	5.7	5.3	2.5	0.7	0.4	7.6	101.8	16	28	138

Note: Samples from this study were analyzed at the Regional Geochemical Center of Saint Mary's University (Halifax, Canada) by X-ray fluorescence (XRF), using a Phillips PW2400 spectrometer via the glass disc fusion method for major elements and pressed powder method for trace elements. Detection limit is 0.1% for major elements, and 1 ppm for trace elements. Dist.: distance; McG: McGillivray Brook Formation; Dunn Pt: Dunn Point Formation; tra.: trachyandesite; pyr-br.: pyroclastic breccia; hor.: horizon.

Table 3: Trace element concentrations in the various lithologies of the Dunn Point, Seaspray Cove, and McGillivray Brook Formations.

d.l. (ppm):	Ba	Co	Ga	Hf	Nb	Rb	Sr	Ta	Th	U	V	W	Zr	Y
	1	0.2	0.5	0.1	0.1	0.1	0.5	0.1	0.2	0.1	8	0.5	0.1	0.1
Sample:														
Q9	368	22.9	19	12.9	48.2	117	89.5	3.1	6.6	2	35	53	528.5	56.4
Q8	707	15	39	15.6	64.1	238	51.2	3.8	8.8	2.5	62	14	675.1	97.2
Q7	363	21	23	10.8	42.8	120	84.6	2.9	5.9	1.6	42	60	476.3	71.4
Q6	369	27.2	24	11.1	43.2	102	35.2	2.7	6.3	1.7	37	51	466.4	50.7
Q5	283	18	24	11.3	44.5	93	68.6	2.9	6.2	1.7	41	66	481.8	55.6
Q4	508	31.9	26	12.5	47.2	82	177	2.9	6.7	1.8	44	55	522.2	57.8
Q3	392	18.7	23	11.9	46.3	45	138.9	2.7	6.5	2.2	47	46	513.5	61.3
Q2	1375	22.4	25	11.6	46.6	42	192	2.7	7	1.8	50	40	508.2	57.6
Q1	178	55.2	25	13.4	49.3	15	87.8	3.2	7.6	2.2	46	94	551.2	59.2
BL08-3**	928	4.0	29.1	19.0	138.0	193.5	42.9	4.8	21.6	8.9	8		1492.4	153.7
BL08-2**	533	3.3	42.1	19.6	175.8	270.1	51.1	5.4	22.4	10.4	9		1913.8	198.4
DPF-05**	1966	0.9	29.7	9.4	65.1	126.8	95.1	2.4	16.9	8.3	6		487.3	104.8
DPF-02**	1695	3.2	28.2	9.0	62.9	121.1	88.3	2.2	16.5	8.4	9		488.2	57.6
GO2*	454			3.1	15.5	9.0	535.0	0.7	1.0				131.0	22.0

d.l. (ppm):	La	Ce	Pr	Nd	Sm	Eu	Gd	Tb	Dy	Ho	Er	Tm	Yb	Lu
	0.1	0.1	0	0.3	0.05	0	0.05	0.01	0.05	0.02	0	0	0.05	0.01
Q9	61.4	127.8	15	63.7	12.8	2	12.6	1.91	10.45	2.15	5.9	0.8	4.9	0.67
Q8	75.1	151	18	76.9	17	4.3	18.26	2.99	17.1	3.51	9.6	1.4	9.08	1.37
Q7	59.2	123.6	15	63.2	13.6	3.1	14.26	2.23	12.36	2.47	6.6	1	5.92	0.9
Q6	46.7	98.2	12	47.9	10.1	1.9	10.95	1.73	9.56	1.98	5.3	0.8	5.02	0.77
Q5	51.4	109	13	56.2	11.5	2.3	11.99	1.89	10.49	2.12	5.8	0.8	5.32	0.79
Q4	56.8	124.2	14	57.6	12.5	2.8	12.47	2.02	11.27	2.25	6.1	1	5.91	0.85
Q3	52.7	113.8	14	56.4	12.4	2.8	12.82	1.99	11.29	2.25	6.1	0.9	5.8	0.85
Q2	49.5	111.1	13	54.6	11.7	2.6	12.04	1.92	10.89	2.16	6	0.9	5.8	0.87
Q1	65	146.9	17	68.9	14.6	3.6	14.21	2.16	11.67	2.17	6.4	0.9	6.07	0.86
BL08-3**	12.2	41.5	5.18	24.4	11.06	0.54	17.38	3.50	23.32	4.60	13.42	2.06	13.6	1.8
BL08-2**	6.7	27.0	3.11	15.8	8.83	0.45	15.36	3.34	23.32	4.60	12.94	1.98	12.5	1.8
DPF-05**	59.9	80.6	13.64	51.4	10.93	0.78	11.64	2.05	13.81	2.86	8.13	1.17	6.7	0.9
DPF-02**	17.3	25.6	4.50	16.3	4.30	0.43	4.86	1.02	7.39	1.61	5.11	0.78	5.3	0.7
GO2*	14.0	33.5	4.59	20.6	5.22	2.00	5.18	0.76	4.92	0.86	2.43	0.33	2.0	0.3

Note: samples from this study were analyzed by inductively coupled plasma mass spectrometry (ICP-MS) at ACME Laboratories (Vancouver, Canada). Results are in parts per million (ppm). d.l.: detection limit (only for the Q samples). *: data from [12]; **: data from Murphy et al. [14].

massive, aphyric to porphyritic, with pseudomorphs of plagioclase altered to calcite and quartz (Figure 7(a)). Phenocrysts occur in a pilotaxitic to mildly trachytic groundmass composed predominantly of quartz, chlorite, and albite. Calcite and quartz amygdules are increasingly abundant going up the profile (Figures 7(b) and 7(c)).

Evidence of moderate paleo-weathering is observed in the ~8-11.5 m interval (samples Q5-9) and is concentrated in vein-like areas characterized by sericitization and hematization (Figure 7(d)). The uppermost ~0.3 m of the *in situ* profile at the Seaspray Cove section (sample Q10) is thoroughly weathered, with no volcanic textures preserved. It is overlain by at least 4 m of sheared paleosol material below the basal tuff of the McGillivray Brook Formation.

6.2. Syn- and Postemplacement Hydrothermal Alteration versus Weathering and Burial Diagenesis. The hydrothermally altered and subsequently weathered trachyandesite profile at Seaspray Cove is composed of albite, orthoclase, quartz, clinochlore, muscovite, carbonates, and hematite, as well as some pyrophyllite near the contact with the overlying tuff (Table 1). Whereas quartz may be produced at all stages of eodiagenesis, we consider albite, clinochlore, and carbonates, which decrease in modal abundance up profile

TABLE 4: Volatile element contents in the Seaspray Cove Formation.

Samples	C-Total (wt.%)	Cl (wt.%)	Mass (g)	F (wt.%)
Detection limit:	0.01	0.01		0.01
Analytical method:	CS	INAA	INAA	FUS-ISE
Q1	0.65	0.04	1.07	0.05
Q2	0.94	0.04	1.01	0.05
Q3	0.82	0.05	1.02	0.05
Q4	1.02	0.05	1.03	0.06
Q5	0.48	0.04	1.06	0.06
Q6	0.21	0.06	1.07	0.06
Q7	0.87	0.02	1.01	0.07
Q8	0.03	0.02	1.06	0.1
Q9	0.22	<0.01	1.01	0.06

Note: concentrations of C, Cl, and F were, respectively, determined by combustion analysis, instrumental neutron activation analysis (INAA), and fusion/ion-selective electrode (Fus-ISE) at Activation Laboratories (Ancaster, Ontario, Canada).

(Figure 8), as the exclusive products of syn- and postemplacement alteration processes that took place in a hotter environment than normal surface temperatures. In contrast, muscovite and hematite modal abundances increase up profile (Figure 8), and these increases are interpreted to be directly proportional to the degree of subsequent weathering, with muscovite contents (as well as pyrophyllite near the contact with tuff) reflecting the original pedogenic clay contents prior to burial. Hence, orthoclase (a minor component of the unweathered rock) and some of the quartz are interpreted as the only unmodified remnants of igneous minerals. Preferential preservation of orthoclase in the weathering profile is consistent with the alkaline weathering conditions that are suggested by the geochemistry of paleosols in the rest of the Ordovician succession at Arisaig [24–26]. Although thoroughly altered during emplacement and cooling, sample Q1 from the base of the profile is the sample in which postemplacement weathering is least significant, as it is characterized by the highest feldspar (~51%) and clinochlore (~17%) contents, and as it is mostly devoid of muscovite (~1%) and hematite (below detection limit) (Table 1). In terms of major element contents, Q1 mainly differs from other samples by its very low K_2O contents (0.4 wt.%). Jutras et al. [24–26] reported substantial K-enrichment in paleosols of the volcanic succession at Arisaig during shallow burial, which is consistent with K_2O contents that increase up profile (Q1-10; Tables 1 and 2) along with modal abundances of weathering minerals in this intermediate rock. Hence, K_2O contents other than those found in orthoclase may reflect the abundance of preburial smectite contents in the profile, which later converted to muscovite and pyrophyllite.

Based on samples S3-7 and S3-8 of Jutras et al. [26] from the preserved uppermost ~2 m of weathered trachyandesite at the Frenchman's Barn northeast section (Figure 4), the upper part of the profile (A horizon) is characterized by the near absence of albite and carbonates (and associated Na_2O and CaO), which indicates thorough weathering in warm and humid conditions. In these samples, modal quartz contents are as low as ~32-45%, but micas and hematite modal contents are as high as ~28-31% and ~21-28%, respectively, (Tables 1 and 2; Figure 8). Because of its quartz-poor and mica-rich mineralogy, this petrified soil horizon is structurally weak, which rendered it susceptible to subsequent faulting (Figure 5).

6.3. Classification. As a consequence of pervasive eodiagenetic overprinting, any classification using elements that are typically mobile in hydrothermal alteration or weathering processes is not reliable for any of the samples. Relatively stable ratios between typically immobile high field strength elements (Ti, Zr, Nb, and Y) in the entire profile suggest that these elements were not significantly affected by these eodiagenetic processes (Tables 2 and 3). Based on its Ti/Zr and Nb/Y ratios (*sensu* [30]), the rock best classifies as a trachyandesite (Figure 9).

6.4. Halogen Contents. With 0.05-0.10 wt.% F and 0.04-0.06 wt.% Cl (Table 4), halogen contents in the trachyandesitic lava flow unit of the Seaspray Cove Formation are high relative to the mantle [31]. In comparison, an average enriched mantle source only has 0.0025% F and 0.0017% Cl [31]. Because halogens can only be leached during hydrothermal alteration and humid climate weathering, and never enriched, their concentrations in the samples are interpreted as remnants of their original contents in the melt.

7. Petrology of the Trachyandesitic Pyroclastic Breccia Unit

The basal pyroclastic breccia of the Seaspray Cove Formation is mostly composed of reddish-grey, pebble-sized clasts with alteration rims within a dark red, gritty matrix. Its original mineralogy was thoroughly altered to quartz (67-70%), albite (8-14%), and clinochlore (3-4%), with further weathering to hematite (7-8%, presumably from the oxic alteration of clinochlore) and muscovite (4-5%, presumably from the diagenetic transformation of clay minerals) (Table 1). Compared with lahar deposits of the same succession, which are products of the sedimentary reworking of more thoroughly weathered material [26], the pyroclastic breccia is characterized by significantly lower modal muscovite and Al_2O_3 contents, and by much higher Na_2O contents (Tables 1 and 2). However, because of its brecciated fabric, moderate weathering is distributed through most of the material, which obscures the nature of the original melt composition.

Some small areas of the breccia's matrix are not oxidized and exhibit well-preserved flow textures (Figure 6(a)). They are also mostly devoid of clasts. However, these nonoxidized areas of the matrix show evidence of Fe-leaching, which seemingly concentrated in the gritty and oxidized surrounding areas (Figure 6(b)) that partly truncate the grey matrix
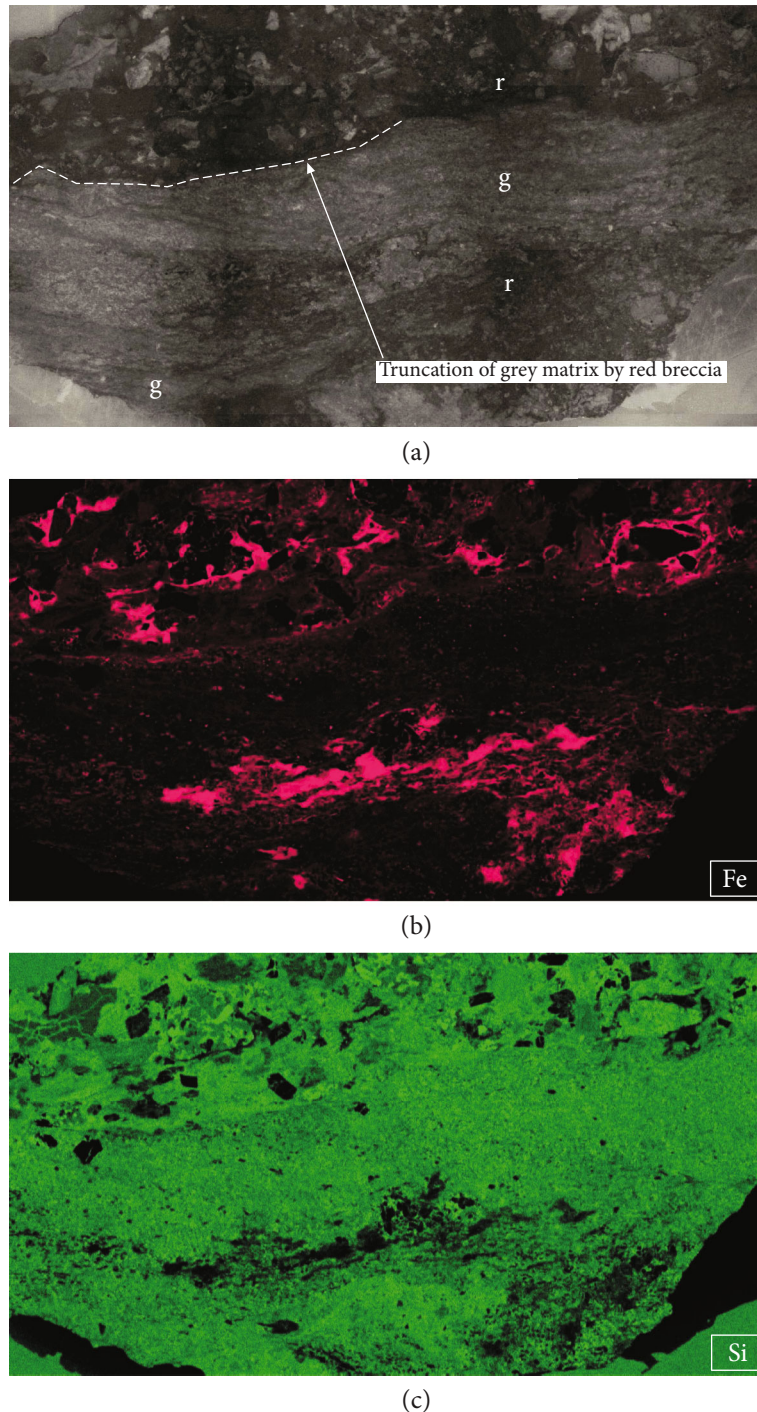
(a)

(b)

(c)

Figure 6: Photo (a) and XRF-element mapping of Fe (b) and Si (c) in one of the rare areas of grey matrix (g) in the basal Seaspray Cove Formation pyroclastic breccia, mingling with a gritty red matrix (r).

(Figure 6(a)). In contrast, the small remnants of grey matrix are slightly richer in Si than the red matrix that forms the bulk of the deposit (Figure 6(c)).

Although similar in SiO_2 concentration to dacite or rhyolite (Table 2), the igneous matrix of the pyroclastic breccia plots in the uppermost range of trachyandesite based on its Zr/Ti and Nb/Y ratios (Figure 9). As its trace element distribution is similar to that of the overlying trachyandesite flow, but in significantly lower concentrations (Figure 10(a)), we conclude that the original magma may have fractionated to a trachyandesitic composition and that SiO_2 enrichment occurred near the top of the magma chamber prior to the eruption, thus diluting the trace element contents without significantly affecting their ratios.
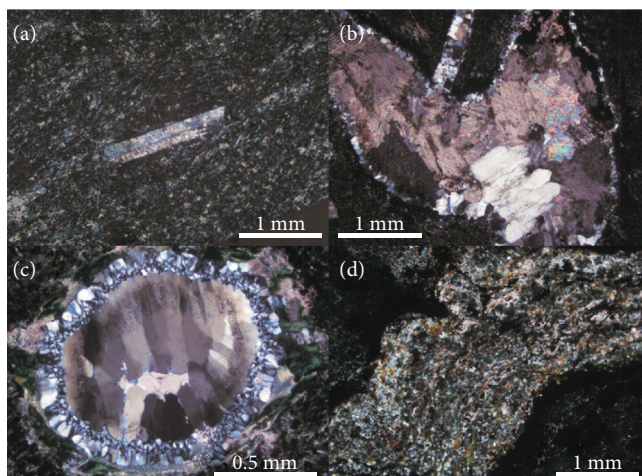
FIGURE 7: Thin-section images from the trachyandesitic lava flow unit of the Seaspray Cove Formation. (a) Plagioclase phenocryst in fine-grained matrix (Q3). (b) Calcite amygdule with minor quartz (Q7). (c) Quartz amygdule with a ring of quartz and chlorite (Q5). (d) Heavily sericitized and oxidized vein-like areas of weathering in the higher part of the trachyandesite profile (Q8).

The inferred Fe-leaching (Figure 6(b)) implies that early alteration processes occurred in reducing conditions and that oxidation occurred subsequently via postemplacement weathering.

8. Zircon Saturation Thermometry

The classic zircon saturation thermometry model developed by Watson and Harrison [32] was calibrated in peraluminous to metaluminous felsic melt compositions. To determine zircon saturation temperatures for a wider range of rock compositions, Gervasoni et al. [33] developed a model using the new bulk compositional parameter G $[(3 \times Al_2O_3 + SiO_2)/(Na_2O + K_2O + CaO + MgO + FeO)]$ against temperature and Zr concentrations, which can also be applied to intermediate and alkaline rocks. Based on data from Table 2, and in accordance with the model of Gervasoni et al. [33], the range of zircon saturation temperatures is 872-887°C in the Dunn Point Formation rhyolite, 765-786°C in the Seaspray Cove Formation trachyandesite (samples Q1-4), and 1065-1103°C in the McGillivray Brook Formation felsic ignimbrite. These results suggest that zircon saturation temperatures determined for the alkaline felsic rocks of the Dunn Point and McGillivray Brook Formation with the model of Watson and Harrison [32] [15] were slightly underestimated.

9. Discussion

9.1. Constraints from the Geology of Peri-Gondwanan Domains in the British Isles. The Leinster–Lakesman, Monian and Cymru terranes of Ireland and England have been variously linked to the Avalonian domain (based on fossil assemblages of their Cambrian to Lower Ordovician rocks; e.g., [17, 34]), or to the Ganderian and Megumian domains (based on lithological similarities and provenance studies; [35, 36]). However, based on similarities in their Ordovician geology, it is generally agreed that these three terranes, along with the Avalonian Wrekin and Charnwood terranes of southern England, were part of the same drifting Ordovician microcontinental assemblage ([36], and references therein), which also included the Avalonian terranes of North America, and which we herein refer to as Avalonia (*sensu* [3, 7, 34, 37]). Hence, the Ordovician successions in the Avalon Zone of North America and in all peri-Gondwanan terranes of the British Isles can be tentatively evaluated in the context of a unified tectonic model for that period.

In the Cymru Terrane and the southern part of the Leinster–Lakesman Terrane, Early Ordovician andesitic arc volcanism is succeeded by Middle Ordovician bimodal back-arc volcanism (Fishguard Volcanic Group and equivalent units), which is interpreted to be the result of slab roll-back, seaward migration of the arc, and crustal stretching in the back-arc region [7, 38]. Near the Middle to Late Ordovician boundary, arc volcanism seemingly migrated back landward and is well recorded in the Duncannon and Borrowdale Volcanic groups of the northern part of the Leinster–Lakesman Terrane [39, 40]. The last volcanic pulse of this subduction zone came at ~454 Ma in the Snowdon Volcanic Group of North Wales, but it is geochemically unrelated to volcanism above a hydrated mantle wedge, and it is interpreted to have occurred when the Iapetan midoceanic ridge partly subducted beneath the arc and opened a slab window in the proximal back-arc region, which was then fed with dry asthenospheric melts ([7], and references therein).

9.2. Petrogenetic Interpretation of Middle to Late Ordovician Igneous Rocks in West Avalonia

9.2.1. Mafic Melts. Based on its higher Nb/Y ratios (Figure 9) and a steeper distribution of rare earth elements (Figure 10(b)), the Seaspray Cove Formation is interpreted as the product of a lower degree of partial melting than the Dunn Point Formation basalts. Ratios of weathering-resistant,
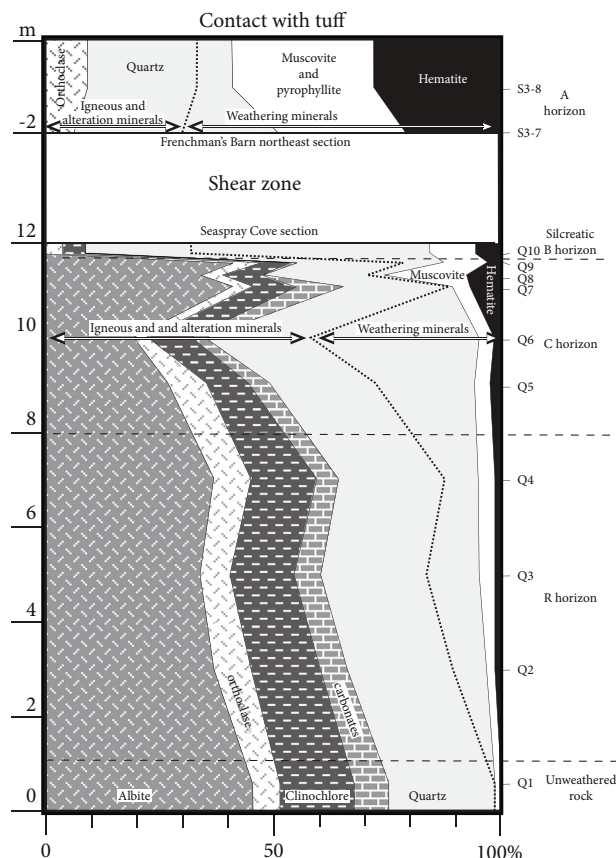
FIGURE 8: Composite section (Seaspray Cove and Frenchman's Barn northeast sections in Figure 1) of the mineral distribution in the McGillivray Brook trachyandesite based on XRD data (Table 1). Albite, orthoclase, clinochlore, and carbonates are considered to be alteration minerals that formed at relatively high temperatures during emplacement and cooling, whereas muscovite and hematite are assumed to have mostly formed during subsequent weathering. Quartz is interpreted to have formed in both environments, but it is assumed that the preweathering quartz contents would have been close to that in the lowermost part of the flow (sample Q1: 24%) and that quartz contents in excess of that would have mostly formed during weathering.

high-field-strength elements (HFSEs) in basalts of the Dunn Point Formation are similar to those of enriched midoceanic ridge basalts (E-MORB; *sensu [41, 42]*; Figures 10(a) and 11), suggesting that they were sourced from depleted upper mantle material enriched over the average (E-DM, *sensu [43]*) and that they were not significantly affected by crustal contamination. Based on the Sm-Nd isotopic characteristics and model ages of these basalts, enrichment of this E-DM source occurred between 1.1 and 0.8 Ga, prior to the oldest rifting event in Avalonia [13, 44]. Melting is interpreted to have occurred at high temperatures through asthenospheric upwelling in a back-arc setting [14, 15] (Figure 12(a)).

In contrast, rocks of the Seaspray Cove Formation show characteristics that are more typical of arc volcanism, such as an intermediate composition, high Cl and F contents (Table 4), relatively pronounced negative Ta-Nb and Ti anomalies (Figure 10(a)), and Th/Yb and Nb/Yb ratios that

plot above the mantle array (*sensu* [42]; Figure 11). Moreover, an estimated zircon saturation temperature of ~786°C indicates low-temperature hydrous melting at the source [45], which is also consistent with an arc setting. In contrast, higher zircon saturation temperature estimates for the more felsic Dunn Point Formation rhyolite (872-887°C) are consistent with high-temperature anhydrous melting in a back-arc setting [15] (Figure 12(b)).

Based on experimental data from Cruz-Uribe et al. [46], alkaline magma with an arc signature can be produced by the partial melting of high-pressure mélanges that occur along the slab-mantle interface, in which subducted altered oceanic crust and sediments are mixed with hydrated mantle-wedge material. Such mélanges are transported into the hot corner of the mantle wedge beneath arcs by low-density mantle-wedge diapirs [47], where their partial melting can feed the arc volcano with alkaline magma [48] (Figure 12(c)).

9.2.2. Evolution towards a Middle to Late Ordovician HFSE-Enriched Intermediate Melt. Although some enrichment in incompatible elements may have occurred due to a low degree of partial melting at the primary source, pronounced negative Eu and Ti anomalies in trachyandesite of the Seaspray Cove Formation (Figure 10(a)) suggest that it was gradually depleted in plagioclase and magnetite through crystal fractionation in the upper part of a magma chamber (Figure 12(c)), which would have favoured further enrichment in incompatible elements. Development of significantly high contents in HFSEs may have been favoured by a high concentration of halogens (Table 4), which tends to be an inherent characteristic of arc volcanism [49], and which enhances the incompatibility of HFSEs by favouring their incorporation into high-order soluble complexes [50–55].

9.2.3. Development of a Late Ordovician HFSE-Enriched Felsic Melt. Although the Seaspray Cove and McGillivray Brook Formations are both strongly enriched in incompatible trace elements, they differ greatly in terms of trace element distribution (Figure 10(b)). As the Seaspray Cove Formation trachyandesite (samples Q1-4) and the McGillivray Brook Formation felsic ignimbrite (samples BL08-2 and BL08-3 from [14]) bear significantly different Th/Hf ratios (0.536-0.603 vs 1.139-1.143; Table 3), the latter is unlikely to be a fractionation product of the former, in accordance with Schiano et al. [56]. Furthermore, the very high melting temperature that is inferred at the source of the McGillivray Brook Formation ignimbrite (~1100°C, based on the model of [33]) implies anhydrous conditions that are incompatible with arc volcanism above a hydrated mantle wedge [15]. However, rocks of such composition can develop in ensialic arc systems in association with the localized development of tensional tectonics [57, 58]. Hence, felsic pyroclastic deposits of the McGillivray Brook Formation are interpreted to represent a different magmatic pulse than intermediate volcanic rocks of the Seaspray Cove Formation, from which it is separated by a prolonged period of weathering.
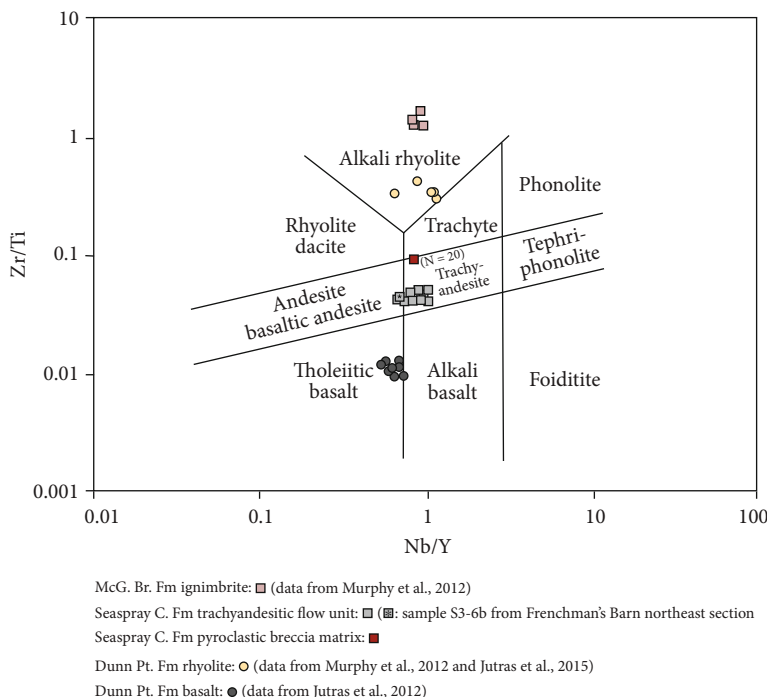
FIGURE 9: Igneous rock classification of the Dunn Point, Seaspray Cove, and McGillivray Brook Formations based on Zr/Ti and Nb/Y ratios (after [30]). Thoroughly weathered samples (Q10, S3-7, and S3-8) are excluded. *N* = 20 refers to the number of averaged point samples from the microprobe (for Ti) and LA-ICP-MS (for Zr, Nb, and Y).

The high trace element contents of the McGillivray Brook Formation ignimbrite may in part be due to a melting temperature that exceeds that of accessory phases in which these elements are concentrated. However, very well developed negative Eu and Ti anomalies (Figure 10(b)) suggest prolonged fractional crystallization in a magma chamber prior to the eruptions. The rocks also show a marked depletion in LREE (Figure 10(b)), which can be attributed to the fractionation of accessory phases such as allanite, monazite or fergusonite in a silicic magma (e.g. [59]).

10. Tectonostratigraphic Setting

Following an Early Ordovician folding episode that was shortly followed by the drifting of Avalonia from Gondwana, arc volcanism is interpreted to have moved outboard in association with steep subduction and slab rollback, and back-arc volcanism developed in currently exposed terranes of both East and West Avalonia in Middle Ordovician times [6, 7, 11, 14, 38, 60] (Figures 12(a) and 13(a)). In East Avalonia, Darriwilian back-arc volcanism is recorded in the bimodal Fishguard Volcanic Group and equivalent units, whereas in West Avalonia, it is recorded in a thick succession of marginally subalkaline within-plate basalts at the base of the Dunn Point Formation (Figures 12(a) and 13(a)), and by the subsequent deposition of thick rhyolite produced by crustal anatexis (Figures 12(b) and 13(b)). The latter records the end of back-arc extension at ~460 Ma. Associated back-arc plutonic activity in the

nearby Antigonish Highlands (Figure 1(b)) is also inferred to have stopped by ~460 Ma [27].

A prolonged period of volcanic quiescence ensued in the West Avalonian region, as indicated by the development of a thick weathering profile in the upper part of the Dunn Point Formation rhyolite [26] and by the 1.4 to 9.6 My (i.e., ~5.5 My) time gap that separates the rhyolite from felsic ignimbrite of the overlying McGillivray Brook Formation based on U-Pb dates from primary zircons [14]. It is within this hiatus that volcanic rocks with an arc-type composition (the new Seaspray Cove Formation) onlapped part of the previously deposited back-arc volcanic succession (Figures 12(c) and 13(c)), pinching-out to the southwest (Figure 3). A similar inboard migration of arc volcanism is recorded in East Avalonia near the Middle to Late Ordovician boundary, juxtaposing arc volcanic rocks of the Duncannon and Borrowdale Volcanic groups with older back-arc volcanic rocks [7, 39, 40]. Because of a lower degree of partial melting at the source and presumably higher halogen contents during crystal fractionation, incompatible HFSE contents are overall greater in intermediate rocks of the Seaspray Cove Formation than in rhyolite of the underlying Dunn Point Formation, despite the latter being significantly more felsic (Table 2; Figure 10).

The lack of a well-defined weathering profile separating the trachyandesitic pyroclastic breccia from the overlying lava flow unit of the Seaspray Cove Formation indicates that these two eruptions were closely spaced in time. The pyroclastic breccia is therefore interpreted as the viscous extrusion of material from the slightly more felsic top of the
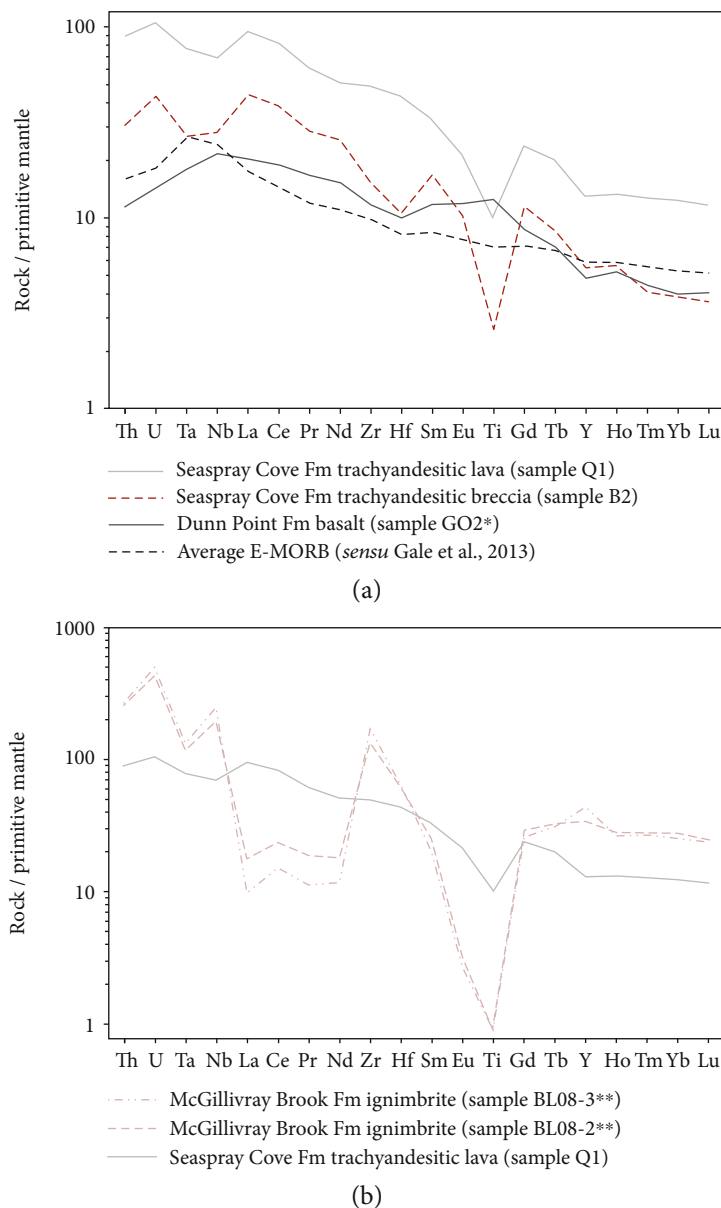
(a)

(b)

Figure 10: Trace element diagrams based on ICP-MS data from Tables 2 and 3 (LA-ICP-MS from Data Repository Files #1 and #2 in the case of the pyroclastic breccia matrix of the Seaspray Cove Formation) and normalized against primitive mantle values from Sun and McDonough [70]. (a) Comparisons between the average enriched midoceanic ridge basalt (E-MORB; based on [41]), the Dunn Point Formation basalts, and the Seaspray Cove Formation trachyandesitic lava flow unit and pyroclastic breccia matrix; (b) comparisons between the Seaspray Cove Formation trachyandesitic flow unit and felsic ignimbrite of the McGillivray Brook Formation. ∗: data from Keppie et al. [12]; ∗∗: data from the least altered samples of ignimbrite analyzed by Murphy et al. [14] based on Na_2O (>1%) and LOI (<1%) contents.

trachyandesitic magma chamber, where water enrichment and silica metasomatism from country rocks may have occurred, and where volcanic pressure was allowed to build. The subsequent eruption of the slightly more mafic trachyandesitic flow was less obstructed and mostly devoid of country rock clasts.

Another prolonged period of weathering separated the emplacement of intermediate lava of the Seaspray Formation from the overlying McGillivray Brook Formation, still within the ~5.5 M.y. interval between deposition of the

~460 Ma rhyolite and the ~454.5 Ma felsic ignimbrite. This blanket of Sandbian felsic pyroclastic rocks marked the end of Ordovician volcanism in West Avalonia (Figures 12(d) and 13(d)).

As noted earlier, the geochemistry of the McGillivray Brook Formation felsic ignimbrite is incompatible with that of the Seaspray Formation and incompatible with arc volcanism above a hydrated mantle wedge. However, the ultrahigh temperature melting of anhydrous crust that sourced these rocks [15] is compatible with slab window magmatism,
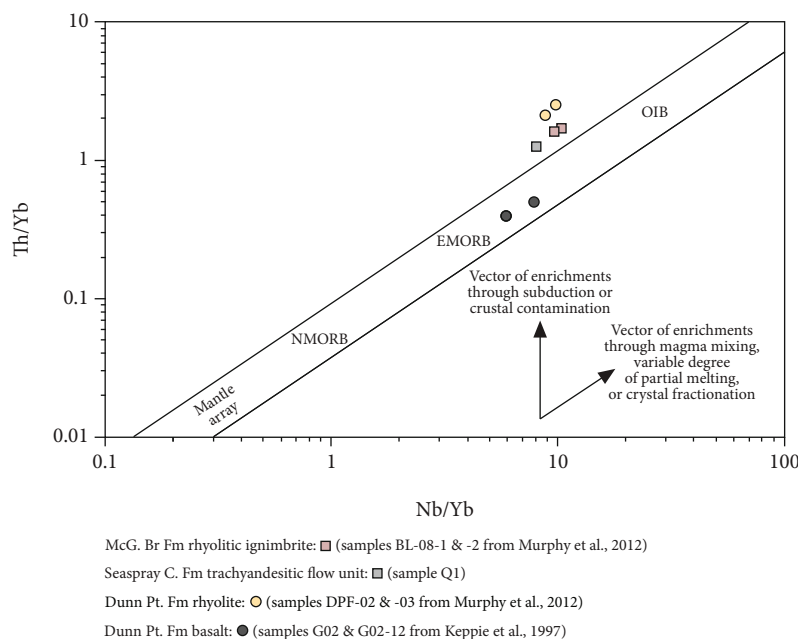
FIGURE 11: Mantle array and vector of subduction and crustal contamination versus that of within-plate, magma mixing, or crystal fractionation enrichments based on Th/Yb and Nb/Yb ratios (after [42]).

which is inferred to have sourced the last pulse of arc-related volcanism along the East Avalonian margin of Iapetus at roughly the same time in the Upper Rhyolitic Tuff Formation of the Snowdon Volcanic Group in north Wales (454.42 ± 0.45 Ma based on U-Pb isotopes from primary zircons; [61]) in association with partial subduction of the oceanic ridge [7] (Figure 12(d)). Furthermore, earlier oceanic ridge subduction beneath the same microplate is inferred to have occurred at the level of Ganderia between 459 and 455 Ma [62] (Figure 13(c)). Oblique convergence of this ridge may have caused its area of subduction to subsequently prograde laterally towards Avalonia (Figures 13(c) and 13(d)). As the shutdown of south-directed subduction beneath Avalonia is roughly coeval with the collision between Ganderia's Popelogan arc and Laurentia farther west along the same subduction zone (~455 Ma according to [56]) (Figure 13(d)), it can be inferred that slab pull of the remaining ocean plate was by then reduced by this obstruction, which could have prevented the Iapetan oceanic ridge from being fully subducted beneath Avalonia.

11. Conclusions

The newly identified trachyandesitic succession of the Seaspray Formation at Arisaig and its stratigraphic relationship with bounding volcanic units of the Dunn Point and McGillivray Brook Formations bring a new perspective on the evolution of the Middle to Late Ordovician magmatic system in West Avalonia, which bears many parallels with the coeval system in East Avalonia. During that time interval, the convergent zone is interpreted to have evolved from steep subduction, rollback, and back-arc extension, to shallower subduction and back-arc shortening (Figure 13). As a result,

Upper Ordovician arc volcanic rocks were juxtaposed with Middle Ordovician back-arc volcanic rocks in East Avalonia [39, 40], and a small outlier of Upper Ordovician arc volcanic rocks (the Seaspray Cove Formation) in West Avalonia eventually onlapped part of the previously deposited Middle Ordovician bimodal back-arc volcanic succession of the Dunn Point Formation (Figure 3). Based on paleocontinental reconstructions showing southward subduction of the Iapetan oceanic lithosphere beneath Avalonia ([1, 5, 7], and references therein), the onlap probably occurred from the north. This interpretation is somewhat consistent with limited field constraints, which suggest that arc volcanic rocks of the Seaspray Cove Formation pinch-out on back-arc volcanic rocks of the Dunn Point Formation towards the southwest (present-day coordinates, Figures 1(b) and 3).

Also noteworthy is the nearly synchronous shutdown of Iapetan subduction in both East and West Avalonia in the late Sandbian (mid-Caradoc) with no significant deformation associated with it (this study and [7]). In East Avalonia, Woodcock [7] attributes the shutdown to an incomplete overriding of the Iapetan oceanic ridge. This hypothesis is consistent with the inferred transition from steep to shallow subduction in Middle to Late Ordovician times beneath West Avalonia, similar to the subduction history of the Nazca Plate [63], which suggests that increasingly young and buoyant oceanic crust was being subducted, and therefore that ano-ceanic ridge may have been gradually approaching the trench (Figures 12 and 13).

In East Avalonia, the last pulse of volcanism associated with the subduction of the Iapetan Ocean plate occurred at ~454.4 Ma and is interpreted as the product of slab window magmatism [7] (Figure 12(d)). Such setting is consistent with the geochemistry of the ~454.5 Ma felsic ignimbrite of the
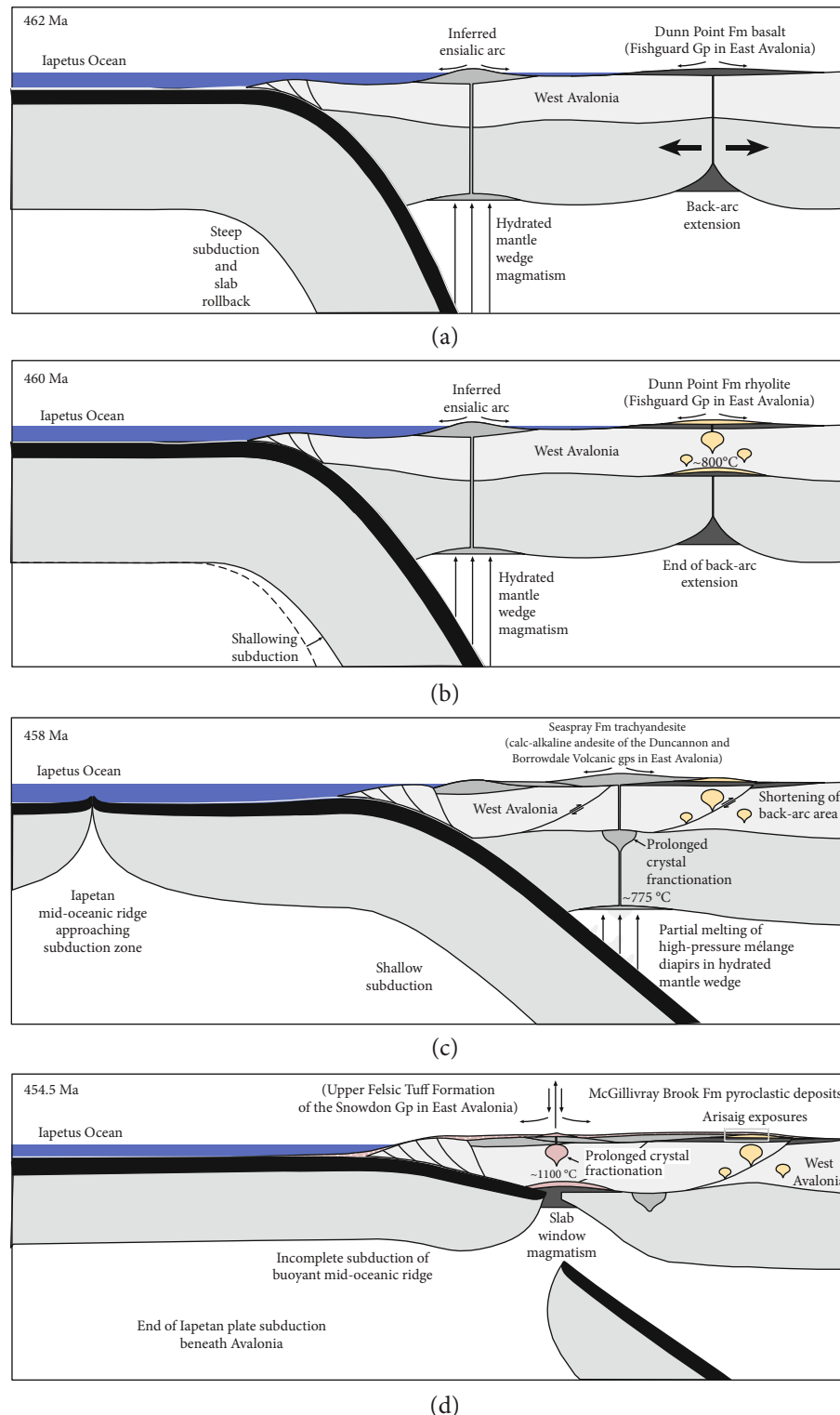
Figure 12: Middle to Late Ordovician tectonic model for West Avalonia, with inferences from the models of (a–b) Murphy et al. [13, 14], (c) Cruz-Uribe et al. [46], and (d) Woodcock [7].

McGillivray Brook Formation, which marked the end of subduction-related volcanism in West Avalonia, and which was sourced from the ultrahigh temperature melting (~1100°C) of anhydrous crust. Such elevated temperatures reaching the base of the crust would be best accounted for

by asthenospheric upwelling associated with the development of a slab window (Figure 12(d)).

The apparent shutdown of subduction beneath both West and East Avalonia in Late Ordovician times suggests that accretion of Avalonia to composite Laurentia during
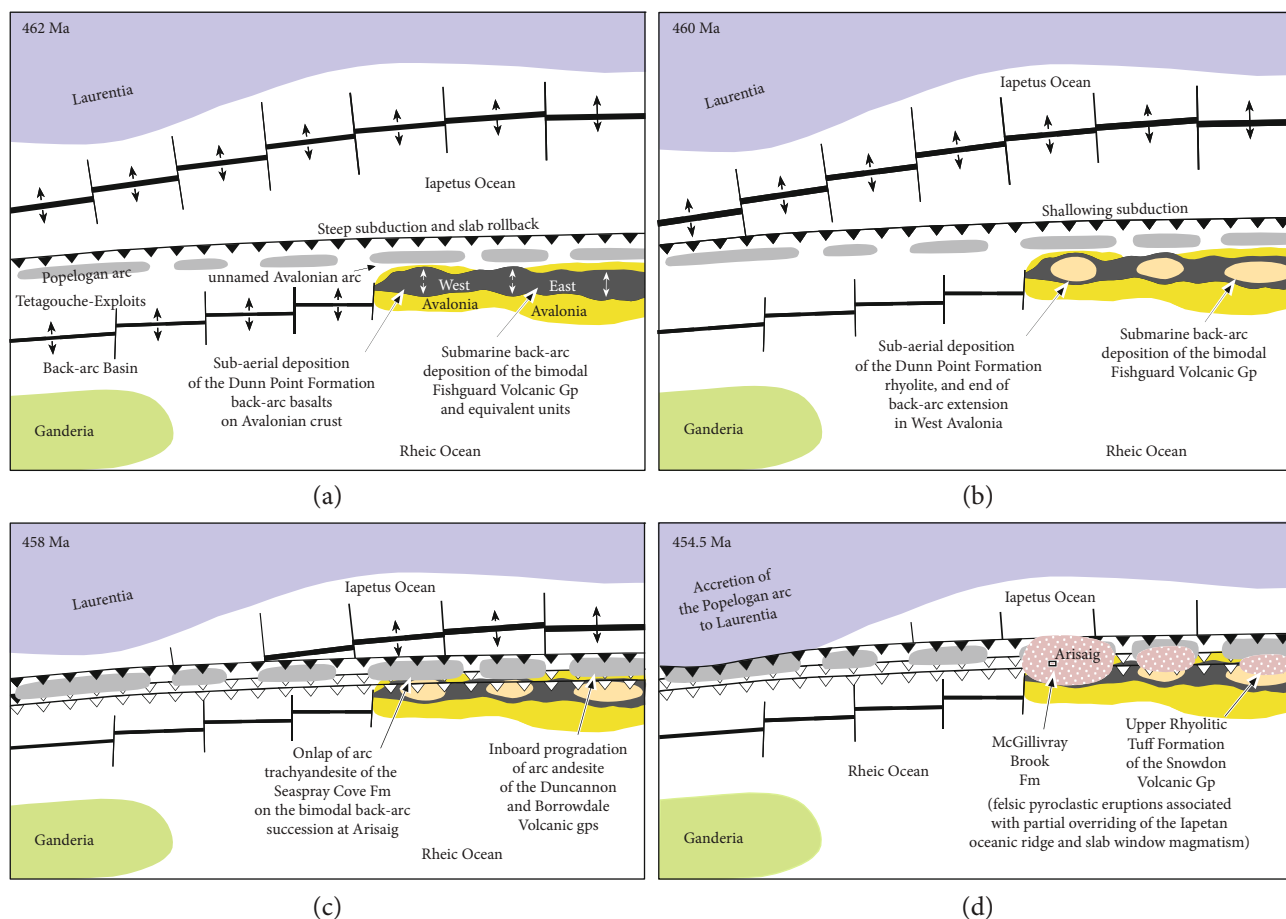
FIGURE 13: Tectonic setting of Ordovician volcanism on West Avalonia in relationship to East Avalonia, Ganderia, and Laurentia. Based on data from Branney and Soper [39], [40], van Staal et al. [6, 62], Murphy et al. [14], Woodcock [7], Phillips et al. [38], Lusty et al. [61], Waldron et al. [35, 36], and this study. Note that East Avalonia corresponds to the East Avalonian/Ganderian assemblage of Waldron et al. [35].

the Devonian (e.g., [6, 60, 64]) occurred through a different subduction zone. This is consistent with the record of Silurian subduction towards the northwest (present-day coordinates) beneath composite Laurentia in Maine [65], which may have gradually consumed the ocean plate remnant that separated the latter from Avalonia at the time (the "Acadian Seaway" of [66]). Intermittent within-plate magmatic activity occurred in Avalonia during this period, but with no association to subduction [67].

Data Availability

All data are included in the manuscript and in two items for the Data Repository.

Conflicts of Interest

The authors declare that they have no conflicts of interest.

Acknowledgments

Supplementary Materials

Supplementary 1. Data Repository File # 1: Electron microprobe data from 20 points in the grey matrix of the McGillivray Brook Formation pyroclastic breccia (sample B2).

Supplementary 2. Data Repository File # 2: LA-ICP-MS data from 20 points in the grey matrix of the McGillivray Brook Formation pyroclastic breccia (sample B2).

References

[1] L. R. M. Cocks and T. H. Torsvik, "Earth geography from 500 to 400 million years ago; a faunal and palaeomagnetic review," *Journal of the Geological Society of London*, vol. 159, no. 6, pp. 631–644, 2002.

[2] J. B. Murphy, S. A. Pisarevsky, R. D. Nance, and J. D. Keppie, "Neoproterozoic–Early Paleozoic evolution of peri-Gondwanan terranes: implications for Laurentia-Gondwana connections," *International Journal of Earth Sciences*, vol. 93, no. 5, pp. 659–682, 2004.

[3] J. B. Murphy, G. Gutierrez-Alonso, R. D. Nance et al., "Origin of the Rheic Ocean: rifting along a Neoproterozoic suture?," *Geology*, vol. 34, no. 5, pp. 325–329, 2006.

[4] C. Scotese, *The Earth System Archive; a spatial-temporal database describing the evolution of the Earth system since the late Precambrian*, International Geological Congress, 2012.

[5] G. M. Stampfli and G. D. Borel, "A plate tectonic model for the Paleozoic and Mesozoic constrained by dynamic plate boundaries and restored synthetic oceanic isochrons," *Earth and Planetary Science Letters*, vol. 196, no. 1-2, pp. 17–33, 2002.

[6] C. R. van Staal, S. M. Barr, and J. B. Murphy, "Provenance and tectonic evolution of Ganderia: Constraints on the evolution of the Iapetus and Rheic oceans," *Geology*, vol. 40, no. 11, pp. 987–990, 2012.

[7] N. H. Woodcock, "Ordovician volcanism and sedimentation on Eastern Avalonia," in *Geological history of Britain and Ireland: Second Edition*, N. H. Woodcock and R. Strachan, Eds., Wiley-Blackwell, 2012, Chapter 10.

[8] J. W. F. Waldron, D. I. Schofield, J. B. Murphy, and C. W. Thomas, "How was the Iapetus Ocean infected with subduction?," *Geology*, vol. 42, no. 12, pp. 1095–1098, 2014.

[9] M. A. Hamilton and J. B. Murphy, "Tectonic significance of a Llanvirn age for the Dunn Point volcanic rocks, Avalon terrane, Nova Scotia, Canada: implications for the evolution of the Iapetus and Rheic Oceans," *Tectonophysics*, vol. 379, no. 1-4, pp. 199–209, 2004.

[10] R. J. E. Johnson and R. Van der Voo, "Pre-folding magnetization reconfirmed for the Late Ordovician-Early Silurian Dunn Point Volcanics, Nova Scotia," *Tectonophysics*, vol. 178, no. 2-4, pp. 193–205, 1990.

[11] J. B. Keppie and J. B. Murphy, "Anatomy of a telescoped pull-apart basin: the stratigraphy and structure of Cambrian-lower Ordovician rocks of the Antigonish Highlands," *Nova Scotia Maritime Sediments and Atlantic Geology*, vol. 24, pp. 123–138, 1988.

[12] J. D. Keppie, J. Dostal, J. B. Murphy, and B. L. Cousens, "Palaeozoic within-plate volcanic rocks in Nova Scotia (Canada) reinterpreted: isotopic constraints on magmatic source and palaeocontinental reconstructions," *Geological Magazine*, vol. 134, no. 4, pp. 425–447, 1997.

[13] J. B. Murphy, J. Dostal, and J. D. Keppie, "Neoproterozoic-Early Devonian magmatism in the Antigonish Highlands, Avalon terrane, Nova Scotia: Tracking the evolution of the mantle and crustal sources during the evolution of the Rheic Ocean," *Tectonophysics*, vol. 461, no. 1-4, pp. 181–201, 2008.

[14] J. B. Murphy, M. A. Hamilton, and B. Leblanc, "Tectonic significance of Late Ordovician silicic magmatism, Avalon terrane, northern Antigonish Highlands, Nova Scotia," vol. 49, no. 1, pp. 346–358, 2012.

[15] J. B. Murphy, J. G. Shellnutt, and W. J. Collins, "Late Neoproterozoic to Carboniferous genesis of A-type magmas in Avalonia of northern Nova Scotia: repeated partial melting of anhydrous lower crust in contrasting tectonic environments," *International Journal of Earth Sciences*, vol. 107, no. 2, pp. 587–599, 2018.

[16] J. B. Murphy, J. D. Keppie, and A. J. Hynes, *Geology of the Antigonish Highlands*, Geological Survey of Canada Paper, 1991.

[17] E. Landing, "Avalon: Insular continent by the latest Precambrian," in *Avalonian and related peri- Gondwanan terranes of the circum–North Atlantic*, R. D. Nance and M. D. Thompson, Eds., vol. 304, pp. 29–63, Geological Society of America Special Paper, 1996.

[18] E. Landing and J. B. Murphy, "Uppermost Precambrian (?)–lower Cambrian of mainland Nova Scotia: Faunas, depositional environments and stratigraphic revision," *Journal of Paleontology*, vol. 65, no. 3, pp. 382–396, 1991.

[19] A. J. Boucot, J. F. Dewey, D. L. Dineley et al., "Geology of the Arisaig area, Antigonish County, Nova Scotia," in *Geology of the Arisaig Area, Antigonish County, Nova Scotia*, vol. 139, Geological Society of America, 1974.

[20] J. D. Keppie, J. Dostal, and M. Zentilli, *Petrology of the Early Silurian Dunn Point and McGillivray Brook Formations*, Nova Scotia Department of Mines Report,, Arisaig, Nova Scotia, 1978.

[21] J. P. Hodych and K. L. Buchan, "Palaeomagnetism of the ca. 440 Ma Cape St Mary's sills of the Avalon Peninsula of Newfoundland: implications for Iapetus Ocean closure," *Geophysical Journal International*, vol. 135, pp. 155–164, 1998.

[22] J. D. Greenough, S. L. Kamo, and T. E. Krogh, "A Silurian U–Pb age for the Cape St Mary's sills, Avalon Peninsula, Newfoundland, Canada: implications for Silurian orogenesis in the Avalon Zone," *Canadian Journal of Earth Sciences*, vol. 30, no. 8, pp. 1607–1612, 1993.

[23] C. R. van Staal and S. M. Barr, "Lithospheric architecture and tectonic evolution of the Canadian Appalachians and associated Atlantic margin," in *Tectonic Styles in Canada: the Lithoprobe Perspective*, J. A. Percival, F. A. Cook, and R. M. Clowes, Eds., pp. 41–95, Geological Association of Canada, 2012, Special Paper, v. 49, Chapter 2.

[24] P. Jutras, R. S. Quillan, and M. J. Leforte, "Evidence from Middle Ordovician paleosols for the predominance of alkaline groundwater at the dawn of land plant radiation," *Geology*, vol. 37, no. 1, pp. 91–94, 2009.

[25] P. Jutras, J. J. Hanley, R. S. Quillan, and M. J. Leforte, "Intrabasaltic soil formation, sedimentary reworking and eodiagenetic K-enrichment in the Middle to Upper Ordovician Dunn Point Formation of eastern Canada: a rare window into early Palaeozoic surface and near-surface conditions," *Geological Magazine*, vol. 149, no. 5, pp. 798–818, 2012.

[26] P. Jutras, M. J. Leforte, and J. J. Hanley, "Record of climatic fluctuations and high pH weathering conditions in a thick Ordovician palaeosol developed in rhyolite of the Dunn Point Formation, Arisaig, Nova Scotia, Canada," *Geological Magazine*, vol. 152, no. 1, pp. 143–165, 2015.

[27] D. B. Archibald, S. M. Barr, J. B. Murphy et al., "Field relationships, petrology, age, and tectonic setting of the Late Cambrian-Ordovician West Barneys River Plutonic Suite, southern Antigonish Highlands, Nova Scotia, Canada," *Canadian Journal of Earth Sciences*, vol. 50, no. 7, pp. 727–745, 2013.

[28] G. H. Brimhall Jr., O. A. Chadwick, C. J. Lewis et al., "Deformational mass transport and invasive processes in soil evolution," *Science*, vol. 255, no. 5045, pp. 695–702, 1992.

[29] D. E. Kelsey, C. Clark, and M. Hand, "Thermobarometric modelling of zircon and monazite growth in melt-bearing systems: Examples using model metapelitic and metapsammitic

granulites," *Journal of Metamorphic Geology*, vol. 26, no. 2, pp. 199–212, 2008.

[30] J. A. Pearce, "A user's guide to basaltic discrimination diagrams," in *Trace element geochemistry of volcanic rocks: applications for massive sulphide exploration*, D. A. Wyman, Ed., vol. 12, pp. 79–113, Geological Association of Canada Short Course Notes, 1996.

[31] W. F. McDonough and S. S. Sun, "The composition of the Earth," *Chemical Geology*, vol. 120, no. 3-4, pp. 223–253, 1995.

[32] E. B. Watson and T. M. Harrison, "Zircon saturation revisited: temperature and composition effects in a variety of crustal magma types," *earth and planetary science letters*, vol. 64, no. 2, pp. 295–304, 1983.

[33] F. Gervasoni, S. Klemme, E. R. V. Rocha-Júnior, and J. Berndt, "Zircon saturation in silicate melts: a new and improved model for aluminous and alkaline melts," *Contributions to Mineralogy and Petrology*, vol. 171, no. 3, article 21, 2016.

[34] L. R. M. Cocks, W. S. McKerrow, and C. R. van Staal, "The margins of Avalonia," *Geological Magazine*, vol. 134, no. 5, pp. 627–636, 1997.

[35] J. W. F. Waldron, D. I. Schofield, S. A. DuFrane et al., "Ganderia-Laurentia collision in the Caledonides of Great Britain and Ireland," *Journal of the Geological Society*, vol. 171, no. 4, pp. 555–569, 2014.

[36] J. W. F. Waldron, D. I. Schofield, G. Pearson, C. Sarkar, Y. Luo, and R. J. Dokken, "Detrital zircon characterization of early Cambrian sandstones from East Avalonia and SE Ireland: implications for terrane affinities in the peri-Gondwanan Caledonides," *Geological Magazine*, vol. 156, no. 7, pp. 1217–1232, 2019.

[37] R. D. M. Nance and J. B. Murphy, "Contrasting basement isotopic signatures and the palinspastic restoration of peripheral orogens; example from the Neoproterozoic Avalonian–Cadomian Belt," *Geology*, vol. 22, no. 7, pp. 617–620, 1994.

[38] B. A. Phillips, A. C. Kerr, and R. Bevins, "A re-appraisal of the petrogenesis and tectonic setting of the Ordovician Fishguard volcanic group, SW Wales," *Geological Magazine*, vol. 153, no. 3, pp. 410–425, 2016.

[39] M. J. Branney and N. J. Soper, "Ordovician volcano-tectonics in the English Lake District," *Journal of the Geological Society*, vol. 145, no. 3, pp. 367–376, 1988.

[40] B. McConnell, "The Ordovician volcanic arc and marginal basin of Leinster," *Irish Journal of Earth Sciences*, vol. 18, pp. 41–49, 2000.

[41] A. Gale, C. A. Dalton, C. H. Langmuir, Y. Su, and J.-G. Schilling, "The mean composition of ocean ridge basalts," *Geochemistry Geophysics Geosystems*, vol. 14, no. 3, pp. 489–518, 2013.

[42] J. A. Pearce, "Geochemical fingerprinting of oceanic basalts with applications to ophiolite classification and the search for Archean oceanic crust," *Lithos*, vol. 100, no. 1-4, pp. 14–48, 2008.

[43] R. K. Workman and S. R. Hart, "Major and trace element composition of the depleted MORB mantle (DMM)," *Earth and Planetary Science Letters*, vol. 231, no. 1-2, pp. 53–72, 2005.

[44] J. B. Murphy and J. Dostal, "Continental mafic magmatism of different ages in the same terrane: Constraints on the evolution of an enriched mantle source," *Geology*, vol. 35, no. 4, pp. 335–338, 2007.

[45] C. F. Miller, S. M. McDowell, and R. W. Mapes, "Hot and cold granites? Implications of zircon saturation temperatures and

[46] A. M. Cruz-Uribe, H. R. Marschall, G. A. Gaetani, and V. Le Roux, "Generation of alkaline magmas in subduction zones by partial melting of mélange diapirs—an experimental study," *Geology*, vol. 46, no. 4, pp. 343–346, 2018.

[47] H. R. Marschall and J. C. Schumacher, "Arc magmas sourced from melange diapirs in subduction zones," *Nature Geoscience*, vol. 5, no. 12, pp. 862–867, 2012.

[48] S. G. Nielsen and H. R. Marschall, "Geochemical evidence for mélange melting in global arcs," *Science Advances*, vol. 3, no. 4, article e1602402, 2017.

[49] G. F. Zellmer, M. Edmonds, and S. M. Straub, "Volatiles in subduction zone magmatism," *Geological Society, London, Special Publications*, vol. 410, pp. 1–17, 2015.

[50] R. D. Congdon and W. P. Nash, "High-fluorine rhyolite: an eruptive pegmatite magma at the Honeycomb Hills, Utah," *Geology*, vol. 16, no. 11, pp. 1018–1021, 1988.

[51] J. Dostal, A. K. Chatterjee, and D. J. Kontak, "Chemical and isotopic (Pb, Sr) zonation in a peraluminous granite pluton; role of fluid fractionation," *Contributions to Mineralogy and Petrology*, vol. 147, no. 1, pp. 74–90, 2004.

[52] N. B. W. Harris, "The role of fluorine and chlorine in the petrogenesis of a peralkaline complex from Saudi Arabia," *Chemical Geology*, vol. 31, pp. 303–310, 1980.

[53] P. Jutras, J. Dostal, and S. Kamo, "Trace element–enriched mid-Visean dikes in the New Carlisle area of Quebec, Canada: Unusual products of a tholeiitic melt sourced from metasomatized mantle rocks and fractionated in a brine-rich upper-crustal environment," *Geological Society of America Bulletin*, vol. 131, no. 11-12, pp. 2079–2093, 2019.

[54] H. Keppler, "Influence of fluorine on the enrichment of high field strength trace elements in granitic rocks," *Contributions to Mineralogy and Petrology*, vol. 114, no. 4, pp. 479–488, 1993.

[55] R. P. Taylor, D. F. Strong, and B. J. Fryer, "Volatile control of contrasting trace element distributions in peralkaline granitic and volcanic rocks," *Contributions to Mineralogy and Petrology*, vol. 77, no. 3, pp. 267–271, 1981.

[56] A. Zagorevski, C. R. van Staal, N. Rogers, V. McNicoll, G. R. Dunning, and J. C. Pollock, "Middle Cambrian to Ordovician arc-backarc development on the leading edge of Ganderia, Newfoundland Appalachians," *Geological Society of America Memoir*, vol. 206, pp. 367–396, 2010.

[57] B. Landenberger and W. J. Collins, "Derivation of A-type granites from a dehydrated charnockitic lower crust: evidence from the Chaelundi Complex, Eastern Australia," *Journal of Petrology*, vol. 37, no. 1, pp. 145–170, 1996.

[58] I. E. M. Smith, B. W. Chappell, G. K. Ward, and R. S. Freeman, "Peralkaline rhyolites associated with andesitic arcs of the southwest Pacific," *Earth and Planet Science Letters*, vol. 37, no. 2, pp. 230–236, 1977.

[59] C. F. Miller and D. W. Mittlefehldt, "Depletion of light rare-earth elements in felsic magmas," *Geology*, vol. 10, no. 3, pp. 129–133, 1982.

[60] C. R. van Staal, J. B. Whalen, P. Valverde-Vaquero, A. Zagorevski, and N. Rogers, "Pre-Carboniferous, episodic accretion-related, orogenesis along the Laurentian margin of the northern Appalachians," *Geological Society, London, Special Publications*, vol. 327, no. 1, pp. 271–316, 2009.

[61] P. A. J. Lusty, A. M. Lacinska, I. L. Millar, C. D. Barrie, and A. J. Boyce, "Volcanological and environmental controls on the

Snowdon mineralization, North Wales, UK: A failed volcanogenic massive sulfide system in the Avalon Zone of the British Caledonides," *Ore Geology Reviews*, vol. 89, pp. 557–586, 2017.

[62] C. R. van Staal, R. A. Wilson, S. L. Kamo, W. C. McClelland, and V. McNicoll, "Evolution of the Early to Middle Ordovician Popelogan arc in New Brunswick, Canada, and adjacent Maine, USA: Record of arc-trench migration and multiple phases of rifting," *Geological Society of America Bulletin*, vol. 128, article B31253.1, 2015.

[63] R. Charrier, V. A. Ramos, F. Tapia, and L. Sagripanti, "Tectono-stratigraphic evolution of the Andean Orogen between 31 and 37°S (Chile and Western Argentina)," *Geological Society, London, Special Publications*, vol. 399, pp. 13–61, 2015.

[64] A. Tremblay and N. Pinet, "Late Neoproterozoic to Permian tectonic evolution of the Quebec Appalachians, Canada," *Earth-Science Reviews*, vol. 160, pp. 131–170, 2016.

[65] A. Piñán Llamas and J. C. Hepburn, "Geochemistry of Silurian–Devonian volcanic rocks in the Coastal Volcanic belt, Machias-Eastport area, Maine: Evidence for a pre-Acadian arc," *Geological Society of America Bulletin*, vol. 125, pp. 1930–1942, 2013.

[66] L. R. Fyffe, S. C. Johnson, and C. R. van Staal, "A review of proterozoic to early paleozoic Lithotectonic Terranes in New Brunswick, Canada and their Tectonic evolution during Penobscot, Taconic, Salinic and Acadian Orogenesis," *Atlantic Geology*, vol. 47, pp. 211–248, 2011.

[67] M. D. Thompson, J. Ramezani, and A. M. Grunow, "Within-plate setting of Paleozoic Alkalic suites in Southeastern New England, USA: Constraints from Chemical Abrasion–TIMS U-Pb Geochronology and Paleomagnetism," *Journal of Geology*, vol. 126, no. 1, pp. 41–61, 2018.

[68] J. Dostal, J. D. Keppie, and R. A. Wilson, "Nd isotopic and trace element constraints on the source of Silurian–Devonian mafic lavas in the Chaleur Bay Synclinorium of New Brunswick (Canada): Tectonic Implications," *Tectonophysics*, vol. 681, pp. 364–375, 2016.

[69] S. M. Bergström, X. Chen, J. C. Gutiérrez-Marco, and A. Dronov, "The new chronostratigraphic classification of the Ordovician System and its relations to major regional series and stages and to δ13C chemostratigraphy," *Lethaia*, vol. 42, pp. 97–107, 2008.

[70] S. S. Sun and W. F. McDonough, "Chemical and isotopic systematics of oceanic basalts: implications for mantle composition and processes," *Geological Society, London, Special Publications*, vol. 42, pp. 313–345, 1989.